Agricultural and Forest Meteorology 174–175 (2013) 85–109

Contents lists available at SciVerse ScienceDirect

Agricultural and Forest Meteorology

journal homepage: www.elsevier.com/locate/agrformet

Review

Tracing the flow of carbon dioxide and water vapor between the biosphere and atmosphere: A review of optical isotope techniques and their application

Timothy J. Griffis*

Department of Soil, Water, and Climate, University of Minnesota-Twin Cities, Soil Science Room 331, 1991 Upper Buford Circle, Saint Paul, MN, USA

ARTICLE INFO

Article history:
Received 21 June 2012
Received in revised form 12 January 2013
Accepted 14 February 2013

Keywords:
Carbon
Eddy covariance
Evapotranspiration
Isotopes
Keeling plot
Kinetic fractionation
Lasers
Leaf water enrichment
Mass spectrometry
Micrometeorology
Photosynthesis
Respiration
Spectroscopy
Water vapor
Scaling issues

ABSTRACT

Development of optical isotope techniques over the last several years has provided scientists a set of tools for tracing the transport and cycling of CO_2 and water vapor between the biosphere and atmosphere. Here, I take a micrometeorological perspective and review these technological advances, assess key instrument performance characteristics, examine how these techniques have been used in the field to improve our understanding of the processes governing the exchange of CO_2 and water vapor, and discuss future research directions. Review of the recent literature indicates that: (1) optical techniques have been used to quantify the isotope composition of biosphere–atmosphere exchange using the traditional Keeling mixing line, flux–gradient, eddy covariance, and chamber approaches under a variety of field conditions with near-continuous data records now extending to more than 5-years; (2) high frequency and near continuous isotope measurements at the canopy scale have demonstrated important new insights regarding the behaviour of kinetic fractionation at the leaf versus canopy scales and the controls on ecosystem respiration that could not have been observed previously using traditional methods; (3) based on the assessment of instrument performance, carbon isotope disequilibrium (the difference between the isotope composition of photosynthesis and respiration), carbon turnover rates, and measurement uncertainties, ^{13}C-CO_2 investigations are best suited for examining the contributions and changes to ecosystem respiration with a need for more innovative ^{13}C-isotope labeling experiments and compound specific isotope analyses under field conditions; (4) significant progress has been made in measuring the oxygen isotope composition of water vapor fluxes and canopy leaf water enrichment. These new data have provided an opportunity to evaluate models of leaf water enrichment and their application to the canopy scale; and (5) the use of ^{18}O-H_2O and ^{18}O-CO_2 as tracers of the coupled carbon–water cycle has matured significantly in recent years. Evidence from a range of ecosystems indicates that ^{18}O-CO_2 disequilibrium (ranging from 0 to 17‰) is much larger than for ^{13}C-CO_2 (typical less than 3‰ in natural C_3 ecosystems) making it a useful tracer of coupled carbon and water cycle processes. However, a better understanding of the role of carbonic anhydrase in photosynthetic and respiratory processes under field conditions is now needed in order to make further progress. Finally, the increasing use and development of isotope-enabled land surface schemes along with the acquisition of high temporal resolution isotope data is providing a new opportunity to constrain the carbon and water cycle processes represented in these models.

Contents

* Tel.: +1 612 625 3117; fax: +1 612 625 2208.
E-mail addresses: tgriffis@umn.edu, timgriffis@umn.edu

0168-1923/$ – see front matter © 2013 Elsevier B.V. All rights reserved.
http://dx.doi.org/10.1016/j.agrformet.2013.02.009

1. Introduction

Elucidating the mechanisms that control the exchange of carbon dioxide (CO_2) and water vapor (H_2O) between the Earth's surface and atmosphere is of fundamental importance to diagnosing changes in the climate system. The development of stable isotope techniques has provided scientists an important set of tools that can be used to gain new insights into the coupled carbon and water cycles on scales ranging from leaf to globe (Keeling et al., 1979; Farquhar, 1983; Francey and Tans, 1987; Farquhar et al., 1989; Tans et al., 1990; Ciais et al., 1995; Yakir and Wang, 1996). Over the last several years there have been significant developments in spectroscopic (optical) isotope measurement technologies that permit high-frequency and near-continuous isotope measurements that are providing new opportunities to quantify and study the processes governing the biosphere–atmosphere exchange. A significant benefit resulting from these new technologies is the potential for broader accessibility and use within the scientific community. This field is changing rapidly and there is already clear evidence that these techniques are providing important observational data for global change research that wasn't possible previously (Bowling et al., 2005; Lee et al., 2009; Wingate et al., 2010a,b; Griffis et al., 2011; Barbour et al., 2011; Welp et al., 2012; Xiao et al., 2012). It would seem timely, therefore, to provide a review of these recent developments and to look forward to new possibilities.

There have been a number of excellent reviews and texts written on stable isotope applications for ecological and atmospheric research (Flanagan and Ehleringer, 1998; Yakir, 2003; Yakir and Sternberg, 2000; Werner et al., 2012) and spectroscopic techniques for atmospheric research (Schiff, 1992, 1994; Werle, 2004; Wagner-Riddle et al., 2005). This review differs in two ways: first, it focuses on state-of-the-art optical isotope measurement methods suitable for biosphere–atmosphere investigations; second, it is written from a micrometeorological perspective with the objective of exploring how isotope flux measurements are being used to increase the scientific understanding of the coupled carbon and water cycles and to help diagnose and constrain important changes taking place within the biosphere–atmosphere.

This article is organized as follows: first, a brief historical perspective regarding the discovery and early use of isotopes is provided for the non-specialist; second, new commercially available optical isotope technologies are reviewed; third, the recent application of isotope flux measurement techniques is assessed; fourth, applications related to biosphere–atmosphere exchange are examined including: flux partitioning (net ecosystem CO_2 exchange and evapotranspiration); factors influencing the temporal variability in the isotope composition of ecosystem respiration; biophysical controls on canopy-scale leaf water enrichment; and the isotopic coupling between water and carbon. Finally, given this developing technology at our disposal I examine some of the emerging opportunities of stable isotope measurements within a network (i.e. FLUXNET or NEON) framework.

Five questions are posed to help frame this review: (1) What sensors are currently available and what are some of the important measurement and calibration issues that have emerged? (2) What have we learned about partitioning fluxes into their components using stable isotope techniques? (3) How have stable isotope techniques been used to help understand the complexities of ecosystem respiration? (4) How have measurements of oxygen isotopes in water vapor and CO_2 provided new insights regarding the coupled carbon and water cycles? and (5) What are some of the key research needs that have evolved from these investigations?

2. Brief historical perspective

Isotopes[1] were discovered in the early 20th century (Soddy, 1913; Thomson, 1913; Urey, 1948). Here our discussion will be limited to the stable light isotopes of carbon, oxygen and hydrogen. These isotopes were discovered in the late 1920s and early 1930s (Giauque and Johnson, 1929a,b; Urey et al., 1932; Nier and Gulbransen, 1939). Application of isotope techniques to problems in environmental science is a relatively young discipline. Alfred Nier's postdoctoral work at Harvard University carefully demonstrated that the carbon isotope abundance ratio of biological and mineral substances varied slightly in nature (Grayson, 1992; Murphey and Nier, 1941; Gulbranson and Nier, 1939). It was through the development of highly sensitive isotope ratio mass spectrometers (IRMS) (Nier, 1947; McKinney et al., 1950) in the late 1930s that helped establish these new lines of observational inquiry and would ultimately lead to new theories and experiments regarding key fractionation processes. The use of stable isotope techniques proliferated as IRMS became more accessible to the broader scientific community.

The mass differences among stable isotopes or isotopologues ultimately provide the opportunity to trace their flow through the biosphere and atmosphere due to kinetic and equilibrium fractionation effects. The fractionation factor (α) is defined as the ratio of the number of two isotopes in one chemical compound (A) divided by the same ratio in a second chemical compound (B) (Hoefs, 1997; Dawson and Brooks, 2001),

$$\alpha_{A-B} = \frac{R_A}{R_B} \quad (1)$$

where, R_A and R_B represent the absolute isotope ratios of compounds A and B. These values can also be represented as a separation factor (deviation from unity) (i.e. $\epsilon = \alpha - 1$). In 1948 Harold Urey introduced "delta" (δ) notation to ensure that the very small variations in isotope ratios, measured by IRMS, were not an artifact of instrument drift (Urey, 1948). It follows, therefore, that

[1] Isotopes are atoms of the same element that have the same number of protons and electrons, but have different numbers of neutrons resulting in a unique atomic mass. Isotopologues are molecules that have a unique isotope composition or number of isotope substitutions.

the isotope composition of a sample is normalized to a reference standard,

$$\delta = \frac{R_s - R_{std}}{R_{std}} \quad (2)$$

where δ is the isotope ratio. This ratio can be multiplied by 10^3 to report the value in parts per thousand (‰). R_s is the sample molar ratio of the heavy (minor) to light (major) isotope and R_{std} is the standard molar ratio. Table 1 summarizes the relative abundance of the isotopologues and the standard scales used for reporting carbon, oxygen, and deuterium isotope ratios (Coplen, 1994, 2011; Dawson and Brooks, 2001). Griffis et al. (2004) show in their appendix A the methodology for converting into and out of delta notation and isotopologue mixing ratios and discuss the origin and importance of the standards used for making these conversions.

In biosphere–atmosphere studies of CO_2 and water vapor exchange we are mainly concerned with kinetic and equilibrium fractionation effects. Kinetic fractionation results from unidirectional and incomplete reactions such as the slower molecular diffusion of the heavy isotopes relative to the lighter isotopes and the slower chemical reaction rates associated with the heavier isotopes. For example, kinetic fractionation associated with the molecular diffusion of ^{13}C-CO_2 relative to ^{12}C-CO_2 through stomata is approximately +4.4‰ and the enzymatic fractionation associated with ribulose 1,5 bisphosphate carboxylase/oxygenase (rubisco) carboxylation of ^{13}C-CO_2 relative to ^{12}C-CO_2 is approximately 29‰ (Farquhar et al., 1989). Therefore, the kinetic effects result in relatively strong photosynthetic fractionation in C_3 plants. This overall fractionation effect is often denoted as Δ and represents the sum of the processes.

Equilibrium (thermodynamic) fractionation results when an isotope exchange takes place between chemical substances, phases, or individual molecules that eventually reach a chemical equilibrium (Hoefs, 1997; Dawson and Brooks, 2001). Here, the heavier isotopes typically accumulate in the compounds or phases that are most dense. For example, the heavy isotope of water (^2H-H_2O and ^{18}O-H_2O) will have relatively higher concentrations in the condensed phase versus the vapor phase due to their lower saturation vapor pressures. While there are mass independent fractionation effects, these are most important for species such as O_3, N_2O, and CO_2 in the stratosphere (Hoefs, 1997; Thiemens, 1999; Kawagucci et al., 2008).

Isotope ratio mass spectrometry (IRMS) separates charged atoms or molecules based on their mass-to-charge ratios and motions in the presence of a strong magnetic field (Dawson and Brooks, 2001). The precision and accuracy of these instruments have been well established over many years of research. IRMS systems have $\delta^{13}C$-CO_2 precision ranging from 0.02 to 0.1‰ and $\delta^{18}O$-CO_2 precision ranging from 0.05 to 0.2‰. High precision IRMS has been paramount in atmospheric inversion type studies that make use of stable isotope measurements utilizing the global flask monitoring network (Trolier et al., 1996; Ciais et al., 1995). Typical precision for δ^2H-H_2O and $\delta^{18}O$-H_2O are 0.5–1‰ and 0.03–0.1‰, respectively (Yakir and Wang, 1996; Lee et al., 2005; Wang et al., 2009).

In some IRMS applications a considerable amount of sample preparation is required offline prior to analysis. In one of the early standard methods of analysis of the deuterium isotope composition of water, it was necessary to first reduce the water sample by zinc to produce hydrogen gas (Coleman et al., 1982; Dawson and Ehleringer, 1991). A couple of points are worth highlighting here. First, it takes about 1-h to prepare 10 water samples for analysis and the preparation requires specialized equipment including a vacuum extraction line. Today, it is more common for IRMS measurements that rely on the reduction of water to use chromium, which can be performed on-line, making the analyses simpler. The oxygen isotope composition of water samples is traditionally determined using the CO_2–H_2O equilibration technique (Cohn and Urey, 1938; Epstein and Mayeda, 1953; Dugan et al., 1985). In this method, the oxygen atoms in water and CO_2 are allowed to equilibrate at 25 °C over a period of 24–96 h and then the CO_2 gas is introduced into the IRMS for analysis.

IRMS are used broadly within the environmental sciences and are well suited for applications that do not require high-frequency information. Their application to *in situ* environmental measurements or micrometeorological investigations, however, are limited mainly because of lack of portability, relatively high cost, sample preparation, and the two-step sampling procedure of flask air sample collection followed by injection into the IRMS. In a typical application, it is not uncommon for a single air sample (flask) to be analyzed over a period of about 10 min. Further, the collection of CO_2 or water vapor in a flask can also introduce sampling errors. This is particularly important for sampling water vapor where the cold trap method is used to freeze out the vapor into a collection flask. If the collection efficiency is not perfect or if the freezing causes homogeneous nucleation then the collected vapor will be positively biased (i.e. too heavy) (Lee et al., 2005; He and Smith, 1999). Despite these challenges and limitations, many investigators have found innovative ways to implement IRMS in micrometeorological applications, but such studies have been limited to short campaigns because of the logistical challenges (Yakir and Wang, 1996; Bowling et al., 1999; Ogée et al., 2004). The cost of analysis can also be substantial, especially for atmospheric applications where the goal is to capture the temporal variability within the flow. If we sampled the atmosphere once per hour at two measurement heights above a canopy over a 1-week measurement campaign the analytical costs could easily exceed $5000 US. A detailed cost analysis for a field experiment where the carbon isotope composition of ecosystem respiration was estimated at high frequency (minutes to hours) using IRMS was estimated at $1.3 M US (Dr. Margaret Barbour, University of Sydney, personal communication). In their application, 960 samples were collected per night to construct 120 Keeling plots over a 1-month period. This involved the collection of 26,880 air samples. The time required for IRMS analysis would have been approximately 1-year of continuous operation. These same analyses can be conducted much faster and at lower analytical costs using optical isotope techniques. The original investment in equipment is still substantial, but is generally lower than the cost of IRMS (Midwood and Millard, 2011). Optical isotope systems range in price from about $50,000 to $150,000 US depending on the species of interest and instrument options.

In addition to lower instrument and sample costs, the use of optical isotope techniques also simplifies some of the sampling methodology such as flask collection and reducing the need for sample preparation prior to analysis. Further, as these methods continue to mature, the high precision and high frequency measurement will allow for micrometeorological theory (first principles) to be applied to land-atmosphere exchange problems so that isotope fluxes can be determined directly.

3. Optical isotope measurement systems

Optical techniques are well suited for determining changes in the chemical composition of atmospheric flows (Schiff, 1992, 1994; Werle, 2004; Wagner-Riddle et al., 2005). Unlike IRMS, optical techniques involve the detection of radiation absorbed and emitted by the target gas species. For a short review of laser-based isotope ratio technology see Kerstel and Gianfrani (2008).

Here, an overview of the two most popular commercially available optical techniques including tunable diode laser absorption spectroscopy (TDLAS) and Fourier-transform infrared (FTIR)

Table 1
Isotope abundance and standard ratios.

Element	Isotope	Ratio measured	Percent abundance	Standard scale	Ratio of standard
Hydrogen	^{1}H $^{2}H(D)$	$^{2}H/^{1}H$	99.985 0.015	V-SMOW	1.55750×10^{-4}
Carbon	^{12}C ^{13}C	$^{13}C/^{12}C$	98.98 1.11	V-PDB	1.11797×10^{-2}
Oxygen	^{16}O ^{17}O ^{18}O	$^{18}O/^{16}O$	99.759 0.037 0.204	V-SMOW or V-PDB	2.0052×10^{-3}, 2.0672×10^{-3}

For additional background information regarding standard scales see Hoefs (1997), Dawson and Brooks (2001), and Coplen (2011). The appendix of Griffis et al. (2004) shows the derivation of the V-PDB carbon isotope ratio and its relation to the original Craig (1957) PDB-Chicago scale. Note that the oxygen isotope ratio can be reported on the V-PDB or V-SMOW scales and that these values can be easily converted from one scale to another. This is important when examining the interaction and equilibration between the oxygen isotopes in water and carbon dioxide.

spectroscopy are reviewed. The TDLAS systems reviewed below all use tunable lasers and an absorption spectrometer to measure an absorption spectrum. The choice of laser type, absorption cell, detection technique, laser stabilization, wavelengths, measurement frequency, etc are all attributes that influence system performance. FTIR is an optical technique, but is fundamentally different than TDLAS in that it does not use a laser source, but rather a broadband blackbody. The basic underlying principles of a number of commercially available systems are reviewed below along with some of their key characteristics, which may help to inform their use in future field applications (Table 2). A common approach to evaluating instrument precision, linearity, and stability has been to sample a set of stable standards over a broad range of mixing ratios and to make use of the Allan variance (Werle et al., 1993; Werle, 2011) to assess how precision changes as a function of time. The results of these types of analyses are presented below and in Table 2. It should be noted that lead-salt tunable diode laser systems (TGA100A, Campbell Scientific Inc., Logan, Utah, USA) were one of the first systems to be used for *in situ* isotope measurements and are regarded here as the benchmark system. However, as of March 2012, the lead-salt diode lasers were no longer being manufactured.

TDLAS has been used for the measurement of atmospheric trace gases for more than 30 years (Edwards et al., 2003). Its fast measurement, high sensitivity, and selectivity made it a viable option for measurement of stable isotopologues of CO_2 (Becker et al., 1992; Crosson et al., 2002; Bowling et al., 2003a) and water (Kerstel et al., 1999, 2002; Gianfrani et al., 2003; Lee et al., 2005).

In general terms this technique is based on detecting the molecular absorption of radiation that is tuned to the rotational–vibrational frequency of the molecule of interest. Isotopologues have unique rotational–vibrational frequencies that can be measured independently provided there is minimal interference from other molecules. The theoretical absorption spectra for a vast number of molecules can be found in the HITRAN database (http://cfa-www.harvard.edu/hitran//) (DeBievre et al., 1984), which can be used to identify non-overlapping absorption lines. Wavenumbers are generally selected that have strong absorption without interference from other molecules. The line width of the laser emission is much less than that of the molecule, making the technique highly selective. In essence, the concentration of the target species can be determined from the Beer–Lambert law (Edwards et al., 2003). One of the challenges associated with isotope applications is the need to measure the concentration of the major and minor isotopologues near-simultaneously. This can be achieved by selecting absorption lines for each isotopologue within a narrow spectral region that can be scanned with a tunable laser.

A commercially available lead-salt TDLAS system (TGA100A and TGA200, Campbell Scientific Inc.) has now been applied at numerous laboratories and field sites for the measurement of CO_2 and water vapor isotopologues (Bowling et al., 2003a, 2005; Griffis et al., 2004, 2005a; Lee et al., 2005; Drewitt et al., 2009; Bickford et al., 2009; Wingate et al., 2010b; Powers et al., 2010; Barbour et al., 2011; Tazoe et al., 2011; Xiao et al., 2012; Welp et al., 2012). One of the most serious drawbacks of using lead-salt diode lasers is the need for cryogens. For some species, such as water vapor, the detectors also need to be cooled using liquid nitrogen. For perspective, a water vapor isotope lead-salt TDLAS system (TGA200, Campbell Scientific Inc., Logan, Utah, USA) consumes about 15 L of LN2 per week. Another important consideration for these systems is to select absorption lines with similar effective line strengths to reduce non-linearity in the isotope ratio (Bowling et al., 2003a; Lee et al., 2005; Griffis et al., 2008, 2010). Further, weaker absorption lines have greater sensitivity to temperature fluctuations. Consequently, it is important to select absorption lines with similar effective line strength and to maintain the instrument at a stable temperature to reduce measurement drift (Bowling et al., 2003a).

The performance of these systems (stability, precision, non-linearity, and reliability) has been well documented for both field and laboratory conditions. Such systems have been operating remotely at the Niwot Ridge USA research station for more than 5 years (Dr. David Bowling, University of Utah, personal communication). The recommended calibration approach for CO_2 isotopologues is to use multiple span values (a minimum 3-point calibration) to account for instrument non-linearity (Bowling et al., 2005). Although the non-linearity for CO_2 isotopologues can be nearly eliminated if the system is properly optimized (Griffis et al., 2008), it remains good practice to calibrate the system using multiple span values that are traceable to long-term laboratory gold standards. Since the fundamental measurement is based on the concentration measurement of each isotopologue (not isotope ratios), the instrument calibration involves the measurement of isotope mixing ratios in standards that have been selected to span the range of expected environmental values (Bowling et al., 2003a; Griffis et al., 2004). Schaeffer et al. (2008) described the long-term precision and accuracy of a TDLAS system for CO_2 isotope measurements operated under field conditions for nearly 2.5 years. Their analyses, based on a 10-min measurement cycle with a 10-s sample duration per sample inlet, resulted in a CO_2 concentration precision of 0.2 $\mu mol\,mol^{-1}$ and a $\delta^{13}C$-CO_2 precision of 0.2‰. Griffis et al. (2005a) showed that the TDLAS measurement precision for $\delta^{18}O$-CO_2 was 0.26‰ for a 2-min measurement cycle and a sampling interval of 30-s. It is important to highlight here that these studies have observed working standards that drifted with time (Griffis et al., 2004; Schaeffer et al., 2008). Therefore, it is good practice to establish a long-term gold standard calibration cylinder, reanalyze working field standards, and to set quality control criteria in post-processing to help identify a subtle drift in the working standards. The recent work of Vogel et al. (2012) outline a robust

Table 2
Overview of optical isotope systems for carbon dioxide and water vapor measurements.

Instrument and model	Isotopologues	Frequency[a]	Stability[b]	Precision[c]	Applications[d]	Comments and key references
Lead-salt tunable diode laser absorption spectrometer (TDLAS) TGA100A/200 Campbell Scientific	^{13}C-CO_2 ^{12}C-CO_2 ^{18}O-CO_2	20 Hz	1–3 h	$\delta^{13}C$-CO_2 0.07 (30 min) 1.8 (20 Hz, 5 Hz passband filter)	Concentration profiles; eddy covariance; automated chambers	No longer manufactured; cryogen required for laser; cryogen required for some detector types; the isotope ratios of water vapor are shown to have strong concentration dependence Bowling et al. (2003b); Griffis et al. (2004); Lee et al. (2005), Schaeffer et al. (2008), Griffis et al. (2008), Wingate et al. (2010b); Powers et al. (2010), Wen et al. (2012), Fassbinder et al. (2012b)
	^{18}O-H_2O ^{1}H-H_2O ^{2}H-H_2O			$\delta^{18}O$-CO_2 0.07 (30 min) 1.4 (20 Hz, 5 Hz passband filter) $\delta^{18}O$-H_2O 0.07 (60 min) 1.6 (10 Hz, 5 Hz passband filter) $\delta^{2}H$-H_2O 1.1 (60 min)		
Wavelength-scanned cavity ring down spectroscopy (WS-CRDS) L1115-i Picarro	^{18}O-H_2O ^{1}H-H_2O ^{2}H-H_2O	0.2 Hz	<200 s	$\delta^{18}O$-H_2O 0.04 (60 min) $\delta^{2}H$-H_2O 0.4 (60 min)	Concentration profiles	Virtually no dependence of δ^2H on concentration; $\delta^{18}O$ bias related to concentration; no cryogen required Wen et al. (2012)
Wavelength-scanned cavity ring down spectroscopy (WS-CRDS) G1101-i and G1101-i+Picarro	^{13}C-CO_2 ^{12}C-CO_2	0.3–0.5 Hz	<2000 s	$\delta^{13}C$-CO_2 0.25 (10 min) $\delta^{13}C$-CO_2 0.08 (30 min)	Automated chambers; long-term (1-year) atmospheric monitoring	Analysis of instrument (G1101-i+) stability and precision reported by Vogel et al. (2012); carbon isotope ratios not dependent on concentration; CH_4 contamination (cross sensitivity) of 0.42‰/ppm Midwood and Millard (2011), Bai et al. (2011), Vogel et al. (2012); Wen et al., (in review)
Off-axis cavity output spectroscopy (OA-ICOS) DLT-100 Los Gatos Research	^{18}O-H_2O ^{1}H-H_2O ^{2}H-H_2O	1 Hz	<200 s	$\delta^{18}O$-H_2O 0.20 (60 min) $\delta^{2}H$-H_2O 0.4 (60 min)	Concentration profiles	Slight dependence of δ^2H and $\delta^{18}O$ on concentration; no cryogen required Wang et al. (2009), Wen et al. (2012)
Off-axis cavity output spectroscopy (OA-ICOS) CCIA DLT-100 Los Gatos Research	^{13}C-CO_2 ^{12}C-CO_2	1 Hz	<200 s	$\delta^{13}C$-CO_2 0.05 (1 min)	Concentration profiles	The carbon isotope ratios are shown to have strong concentration dependence over the range of 300–2000 ppm McAlexander et al. (2011), Guillon et al. (2012); Wen et al., (in review)
Quantum cascade laser absorption spectrometer (QCLAS) Aerodyne research	^{13}C-CO_2 ^{12}C-CO_2 ^{18}O-CO_2	10 Hz	<100 s	$\delta^{13}C$-CO_2 0.1 (30 min) 0.54 (10 Hz) $\delta^{18}O$-CO_2 (30 min) 0.62 (10 Hz)	Eddy covariance; automated chambers	Cryogen required for detectors; cryogen-free design also available Saleska et al. (2006), Tuzson et al. (2008); Kammer et al. (2011); Sturm et al. (2012)
Fourier transform infrared spectrometer (FTIR), Trace gas analyzer Ecotech Pty Ltd.	^{13}C-CO_2 ^{12}C-CO_2	1 Hz	>1 h	$\delta^{13}C$-CO_2 0.03 (10 min)	Concentration profiles; automated chambers	Water vapor isotopologue measurements currently being tested; preliminary results show strong dependence of δ^2H and $\delta^{18}O$ on concentration Haverd et al. (2011), Griffith et al. (2012)
	^{18}O-H_2O ^{1}H-H_2O ^{2}H-H_2O And other species			$\delta^{18}O$-H_2O 0.2 (30 min) $\delta^{2}H$-H_2O 0.5 (10 min) at 20 mmol mol^{-1} 3 (10 min) at 3 mmol mol^{-1}		
Fourier transform infrared spectrometer (FTIR), Nicolet Avatar 370, Thermo Electron, USA	^{13}C-CO_2 ^{12}C-CO_2	0.23 Hz	<960 s	$\delta^{13}C$-CO_2 0.15 (16 min)	Concentration profiles	Performance highly sensitive to air sample temperature and pressure; cryogen required for detector Mohn et al. (2008)

Note that all systems reviewed above, excluding FTIR, are defined as TDLAS techniques.

[a] This value represents the maximum measurement frequency and should not be interpreted as the instrument response time.

[b] Stability was determined using the Allan variance technique.

[c] These values represent the precision after calibrations have been applied. The number in parentheses indicates the averaging interval. Note that some of the precision estimates are concentration dependent.

[d] Configuration of analyzer in field experiments published in the literature.

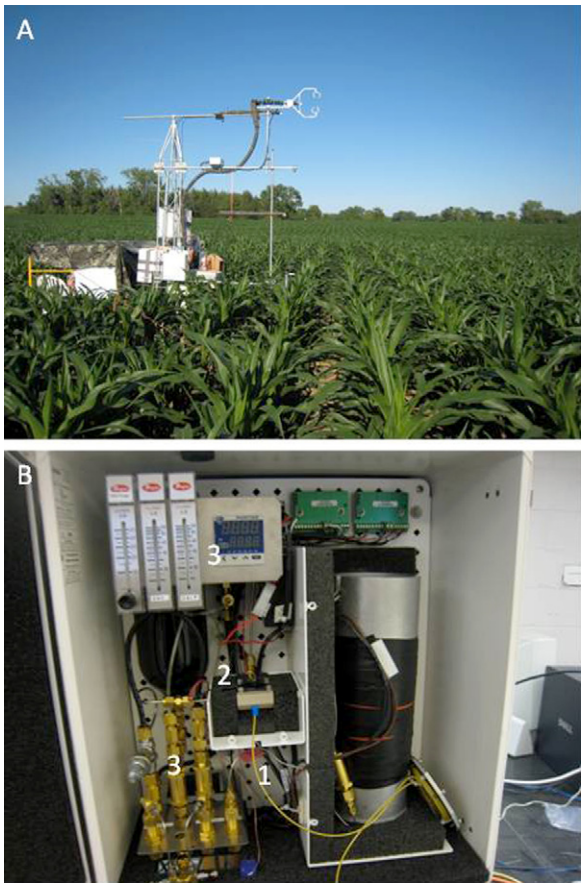

Fig. 1. (A) Photograph of the first eddy covariance water vapor isotope system installed at the Rosemount Research and Outreach Center at the University of Minnesota. Isotope flux measurements of ^{18}O-H_2O and H_2O were measured above a corn canopy using a sonic anemometer and TDLAS approach (TGA200, Campbell Scientific Inc.) during summer 2009 and (B) photograph of the dripper calibration system illustrating the laminar flow tube (1), evaporating hot plate (2), and the flow controls for mixing dry air and water vapor (3). In this approach the dripper rate is controlled by adjusting the pressure of the calibration water reservoir.

strategy of using short, medium, and very long-term standards as part of Environment Canada's isotope and trace gas measurement program.

The lead-salt TDLAS system used to measure water vapor isotopologues (H_2O, ^{18}O-H_2O, ^{2}H-H_2O) has been shown to be highly non-linear with the isotope ratio varying as a function of the total water vapor concentration. Lee et al. (2005) were the first to use a syringe pump, an evaporation plate, and ultra-dry air to generate calibration span gases having a constant isotope ratio equal to the source water. In this approach the calibration strategy is to closely bracket (to within 10%) the observed ambient water vapor mixing ratios in order to minimize the non-linearity issue. Griffis et al. (2010) used a similar analyzer, but re-engineered for the eddy covariance application, also showed that the oxygen isotope ratio varied by about 1‰ per mmol mol^{-1} of water vapor. In their calibration approach the dripper system consisted of a 650 ml water reservoir and used a pressure drop laminar flow tube and compressed dry air to provide a controlled drip rate on to an evaporating plate (Fig. 1). More recently, Rambo et al. (2012) have demonstrated a nebulizer-based approach (Water Vapor Isotope Standard Source, Los Gatos Research, Mountain View, CA, USA) that can provide a robust long-term calibration source. Each of these calibration strategies approached the problem by using a constant isotope ratio, but for a range of mixing ratios targeting the ambient variations.

Wen et al. (2012) have examined the calibration precision and stability of four different commercially available water vapor isotope analyzers. In their analysis of the TGA100A, they concluded that the oxygen isotope ratio had greater sensitivity to total mixing ratio than the deuterium isotope ratio. Further, they showed that the calibration precision decreased as total water vapor mixing ratio decreased. As noted above for CO_2 isotope measurements, it is the mixing ratio span values that are critical to the precision and performance of spectroscopy measurements not the isotope ratios. Therefore, "delta stretching", which results from the mismatch in delta value between the calibration source and sample (an important consideration in IRMS measurements) is not significant here because the fundamental measurement is the mixing ratio. A 1-h precision for the TGA100A measurement of $\delta^{18}O$-H_2O and $\delta^{2}H$-H_2O has been reported to be 0.07–0.12‰ and 1.1–2.0‰ (Lee et al., 2005; Wen et al., 2008, 2012).

The calibration and measurement stability of the analyzer is another important consideration for making reliable field measurements. One of the standard approaches for assessing measurement stability is the Allan variance (Werle et al., 1993; Werle, 2011). Griffis et al. (2008) used this method to examine the stability of the calibration measurements (gain factors) for a TGA100A CO_2 isotope system that was maintained in the field. Their analyses indicated that the Allan variance remained at or below the initial value for a period of about 3-h, suggesting that the calibration interval could be extended out to about 3-h. Wen et al. (2008, 2012) have shown that the calibrated TGA100A water vapor isotope measurements continue to improve beyond an averaging interval of about 1-h. Thus, these systems have been shown to be relatively stable over averaging intervals that are suitable for environmental and micrometeorological measurements under field conditions.

Cavity ring-down spectroscopy (CRDS) uses a continuous wave laser and measures the rate of change in absorbed radiation of laser light that is temporarily "trapped" within a highly reflective sample cell (optical cavity). This technique is used to compensate for the weak molecular absorption in the near IR (Wahl et al., 2006). In essence, the near IR laser emission builds up in the cavity when the laser is turned on until it reaches a critical threshold detected by a photo-detector. The laser is turned off upon reaching the threshold value and the decay time required for light to escape the cell is measured. This decay is exponential and related to the fact that the mirrored sample cell does not have perfect reflectivity. In the presence of a target gas species the decay rate increases because light is lost due to gas absorptivity. This accelerates the decay time ("ring down"). Wahl et al. (2006) described an early version of CRDS for ^{13}C-CO_2 measurements at very high (4%) concentrations. In their system, the physical cell length was 0.20 m and yielded a round-trip effective path length of about 8 km. Their estimate of precision for this CRDS system was 0.2‰ based on repeated samples over a period of 78-min. TDLAS systems based on this general approach have now been developed for measuring ambient atmospheric CO_2 and H_2O (vapor and liquid) isotopologues. A related technique makes use of off-axis integrated cavity output spectroscopy (OA-ICOS, Los Gatos Research) (Wang et al., 2009). Here, an off-axis trajectory of the laser beam, with respect to the optical cavity, is used to prevent light from interfering with itself in the cavity (a problem known as cavity resonance).

To date, very few studies have used OA-ICOS or CRDS systems for CO_2 isotope measurements and their is limited information (i.e. aside from the manufacturers) regarding their stability and precision under lab or field conditions. Recent work by Midwood and Millard (2011) and Bai et al. (2011) have used CRDS (G1101-i, Picarro, Sunnyvale, California, USA) systems for determining the isotope composition of soil respiration using chamber techniques. However, their studies provided few details regarding a systematic test based on Allan variance for the stability and precision of

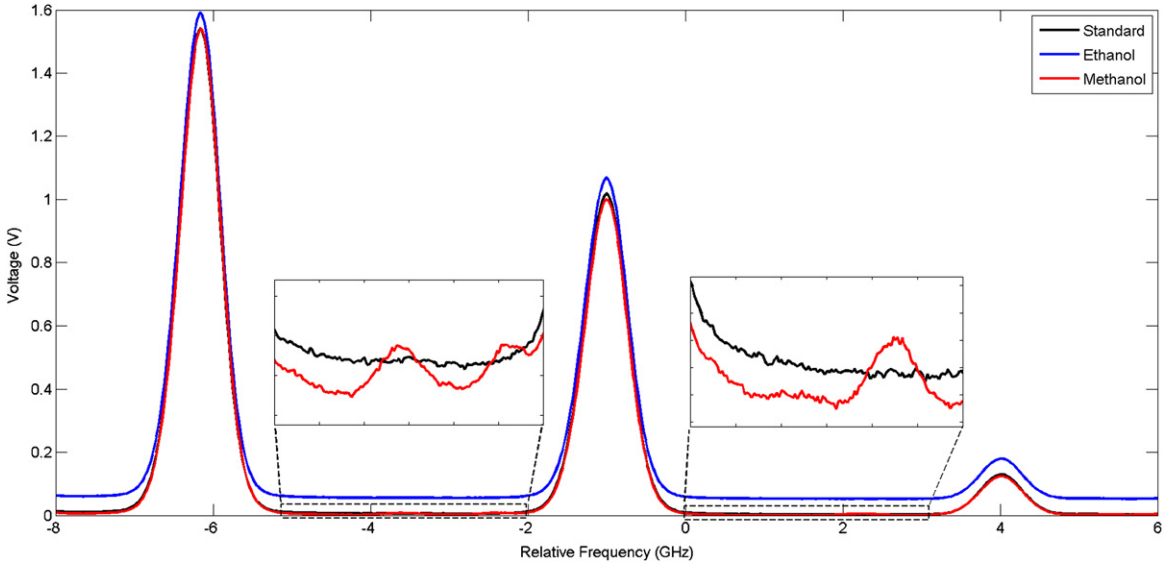

Fig. 2. Illustration of spectral contamination by ethanol and methanol in a liquid water sample using an optical isotope technique. This example demonstrates how the OA-ICOS (DLT-100, Los Gatos Research) archiving and post-processing of spectra can be used to identify contamination in water samples. The zoomed sections (insets) show the contamination problem related to methanol. In this example, a water sample with methanol contamination causes a peak in the voltage above the pure water sample. See Schultz et al. (2011) and Leen et al. (2012) for further details regarding the correction procedure.

the CRDS system. Recently, Vogel et al. (2012) evaluated the latest version of this analyzer (G1101-i+) over a 1-year period and made direct comparisons with Environment Canada's IRMS system. They concluded that the repeatability for δ^{13}C-CO_2 was 0.25‰ for a 10-min measurement interval and improved to 0.15‰ for a 20-min interval. They observed no concentration dependence of δ^{13}C-CO_2 over a range of 303–437 μmol mol^{-1}, but detected a cross-sensitivity to CH_4 of 0.42‰ ppm^{-1}. They concluded, based on long-term measurements of a target gas, that calibration every 7 h yielded a reproducibility of about 0.18‰ and showed excellent agreement (i.e. within 0.002‰) of their IRMS measurements over a period of 1-year. Wen et al. (2013) using a similar analyzer (model G1101-i) have shown that the Allan variance stays at or below its initial value to just over 30-min.

McAlexander et al. (2011) and Guillon et al. (2012) have used an OA-ICOS system (CCIA DLT-100, Los Gatos Research) as a means of detecting geological CO_2 sequestration leakage. Based on the Allan variance analysis, Guillon et al. (2012) have demonstrated that δ^{13}C-CO_2 precision for their system was 0.05‰ for an averaging time of 1-min. In their experiments they were working with very high CO_2 concentrations ranging from 1920 to 17,800 ppm. They noted that the δ^{13}C-CO_2 value was concentration dependent and highly non-linear over the range of 300–2000 ppm and that the analyzer stability was also very sensitive to temperature.

Wen et al. (2012) have provided a comprehensive comparison of the above techniques for water vapor measurements. Examination of Allan variance behavior among analyzers for un-calibrated and calibrated signals indicated that the CRDS and OA-ICOS systems had better stability and precision for the uncalibrated raw signal than the lead-salt TDLAS systems (TGA100A). However, the calibrated lead-salt TDLAS and CRDS signals showed significantly improved precision and stability for longer averaging intervals. Thus, more frequent calibration could be used to improve the precision of the measurement. Their experiment also evaluated the concentration dependence (non-linearity) of the CRDS and OA-ICOS systems. While both systems exhibited little dependence of δ^2H-H_2O on water vapor concentration/humidity, both systems showed that δ^{18}O-H_2O was strongly sensitive to humidity values. For instance, at water vapor mixing ratios of 1.5 mmol mol^{-1} the δ^{18}O-H_2O values were biased by up to 3‰. Again, highlighting the importance of closely bracketing the ambient mixing ratio with appropriate span values for each of these analyzers. The precision of these systems was also evaluated and generally showed no dependence on humidity. Hourly precision values for δ^{18}O-H_2O and δ^2H-H_2O ranged from 0.18 to 0.20‰ and 0.4 to 0.4 for CRDS and OA-ICOS, respectively.

CRDS and OA-ICOS systems are now being used routinely to measure the oxygen and hydrogen isotope composition of liquid water samples (precipitation, ground water, soil water, plant water, etc.) (Herbstritt et al., 2012). These systems provide fast and accurate isotope analysis of pure water samples with a precision comparable to IRMS (Brand et al., 2009; West et al., 2010). However, there is growing evidence that water samples containing organic molecules such as methanol and ethanol can cause significant contamination and large errors in spectroscopy-based methods (West et al., 2010; Zhao et al., 2011; Schultz et al., 2011). Schultz et al. (2011) and Leen et al. (2012) have demonstrated that this spectral contamination can be identified and corrected using post-processing software developed for the OA-ICOS system (Fig. 2). An important recommendation is the need for routine cross comparisons with IRMS and analyzer-specific corrections based on ethanol and methanol standard curves that are likely to vary over time.

Mid-infrared quantum cascade lasers (QCL) have become more affordable over the last several years and increasingly incorporated into TDLAS systems. A major advantage of QCLs is that they have stronger power output and can be operated at near-room temperature with no need for cryogens, representing a significant advantage for remote field applications. Saleska et al. (2006) described a prototype pulsed near-room temperature QCLAS system (Aerodyne Research Inc., Billerica, Maine, USA) for CO_2 isotope measurements at wavenumbers of 2310–2315 cm^{-1}. In their system, a dual path multi-pass cell (astigmatic Herriott cell) was used to measure near simultaneous absorption of ^{13}C-CO_2 and ^{12}C-CO_2. In this multi-pass approach, similar absorption line strength was maintained between the isotopes reducing problems of non-linearity. Tuzson et al. (2008) evaluated the performance of this cryogen-free system under laboratory and field conditions and demonstrated 1 s precision for δ^{13}C-CO_2 and δ^{18}O-CO_2 of 0.3‰ and 0.03 and 0.05‰ at an integration time of 100 s. More recently, Sturm

et al. (2012) tested a commercially available version of this system for eddy covariance isotope flux measurements of ^{13}C-CO_2, ^{12}C-CO_2, and ^{18}O-CO_2. This analyzer used a 300 ml volume sample cell with path length of 7.3 m and liquid nitrogen cooled detectors. Allan variance tests indicated that the system was relatively stable for averaging periods out to about 100 s. The 0.1 s precision for $\delta^{13}C$-CO_2 was 0.6‰ and 0.06‰ at 100 s. The precision decreased (i.e. the instrument noise increased) to about 0.1‰ at 30 min – a typical averaging interval for eddy covariance measurements.

FTIR spectrometers have been commercially available for decades. They are able to take advantage of the stronger molecular absorption in the mid-infrared wavebands using a broadband source instead of an expensive laser diode. Compared to TDLAS, FTIR instruments measure a much wider spectral range, but with much lower resolution. A major advantage of this technology is the simultaneous retrieval of many species. The University of Wollongong FTIR trace gas analyzer (now manufactured by Ecotech Pty Ltd., Knoxfield, Victoria, Australia) has been deployed in the laboratory and field and used to measure a broad range of species including CO_2, CH_4, CO, N_2O, ^{13}C-CO_2, ^{18}O-H_2O, and ^{2}H-H_2O at relatively high precision (Esler et al., 2000; Griffith et al., 2006, 2012). This system consists of an interferometer, multipass cell, and a thermoelectrically cooled detector to measure the absorption spectrum for the molecules of interest in the 1800–5000 cm^{-1} region with a maximum 1 cm^{-1} resolution (Griffith et al., 2012). The measured spectra are archived in realtime and fitted to model spectra from the HITRAN database using a linear or non-linear least squares fitting procedure. Mixing ratios are derived from this fitting procedure, which takes into account sample cell temperature and pressure. The spectral region, 2150–2320 cm^{-1} has been used to determine the ^{13}C-CO_2 and ^{12}C-CO_2 mixing ratios. Allan variance analysis demonstrated that the $\delta^{13}C$-CO_2 precision was 0.07‰ for spectral acquisition times of about 1-min, 0.03‰ at 10-min, and continued to improve to about 0.01‰ at 100-min (Griffith et al., 2012). Results from a 3-month field campaign demonstrated that the analyzer was stable and that calibration once per day was sufficient to account for instrument drift. Recent measurements of water vapor isotopologues (H_2O and ^{2}H-H_2O) in the 3600 cm^{-1} and 2800 cm^{-1}, respectively, show significant promise for routine water vapor isotope measurements (Dr. David Griffith, University of Wollongong and Dr. Stephen Parkes, Institute for Environmental Research, Australian Nuclear Science and Technology Organisation (ANSTO), personal communication). Haverd et al. (2011) have recently demonstrated that this FTIR system could be used to obtain forest canopy profiles of $\delta^{2}H$-H_2O with a 10-min precision on the order of 3‰. Further testing of this system for $\delta^{18}O$-H_2O is ongoing.

The Ecotech FTIR system has performance characteristics that are suitable for *in situ* measurement, tall tower applications, and micrometeorological approaches such as flux–gradient, conditional sampling, and the eddy disjunct approach. The current practical upper limit on measurement frequency is about 1 Hz. At this sample rate the spectra cannot be analyzed in realtime. Since it takes 10–15 s to fit 3 spectral windows it would take approximately 2 weeks to fit all of the spectra for a full day of 1 Hz measurements. Innovations with respect to the spectral fitting procedure could allow for direct eddy covariance measurements. Until then, applications related to flux–gradient, conditional sampling, and the eddy disjunct approach should be feasible.

Mohn et al. (2008) have also demonstrated that a commercially available FTIR system (Nicolet Avatar 370, Thermo Electron, USA) can provide precise and stable $\delta^{13}C$-CO_2 measurements under field conditions. In their approach, a partial least-squares algorithm and use of multiple calibration standards were used to help obtain precise ^{12}C-CO_2 and ^{13}C-CO_2 concentrations within the 2265.7–2304.0 cm^{-1} spectral region. Although they showed a strong dependency of $\delta^{13}C$-CO_2 on the sample gas temperature (14‰/K)– this effect was minimized by precising controlling the sample air temperature and pressure prior to analysis. Allan variance analyses showed that this system yielded a maximum precision of about 0.15‰ at an integration time of 16-min. Further, when comparing the *in situ* measurements with flask samples and IRMS analysis they demonstrated that the overall accuracy of the FTIR system was better than 0.4‰, showing considerable promise for routine field measurements.

4. Canopy-scale isotope flux measurements

There are a number of reasons for developing the capacity to measure isotope fluxes of CO_2 and water vapor between Earth's surface and the atmosphere. Flux information is needed at the canopy scale because of the strong heterogeneity inherent in both water and carbon pools. Even within agricultural lands, that are traditionally viewed as homogeneous, significant spatial variability in the oxygen and deuterium isotope composition of soil water and variation within the vertical isotope distribution of leaf water is observed (Welp et al., 2008; Griffis et al., 2011). It has now been shown that the isotope fractionation factors acting at the leaf scale can behave differently at the canopy scale (Lee et al., 2009). Investigators have been motivated to partition canopy-scale fluxes such as evapotranspiration (ET) and net ecosystem CO_2 exchange (F_N) into the component fluxes using isotope-based approaches. Further, canopy scale isotope flux information can be used as a diagnostic of the processes represented in land surface schemes (Xiao et al., 2010; Riley et al., 2002, 2003). As with other scalars such as water vapor, sensible heat, and CO_2, it is highly desirable to measure the isotope fluxes from first principles. Eddy covariance represents an important example where theory based on first principles and advances in measurement technologies have made a major impact on data acquisition and an understanding of the global carbon and water cycles (Baldocchi, 2008; Jung et al., 2010). However, at the present time, most investigations of canopy-scale water vapor and CO_2 isotopic exchange have used indirect approaches such as the Keeling mixing model (Keeling, 1958; Pataki et al., 2003; Zobitz et al., 2006) because fast and precise measurement of the isotopologues had not been readily available.

A number of inherent limitations have been identified with the Keeling method. First, there is likely to be more than two end members contributing to the variations observed in the atmospheric boundary layer. Keeling plot analyses of ^{18}O-H_2O and ^{18}O-CO_2 have shown that this two end member assumption is often violated because of substantial differences in the signals between soil and vegetation (Amundson et al., 1998; Sternberg et al., 1998; Mortazavi and Chanton, 2002; Bowling et al., 2003b; Ogée et al., 2004). In a recent study involving an isotope-enabled large-eddy simulation model, Lee et al. (2012) demonstrated that the Keeling plot estimates were severely biased because of top-down diffusion (entrainment, which represents another end member). The Keeling method was particularly unreliable for water vapor, because of the strong gradient and differences in isotope composition across the top of the atmospheric boundary layer. Further, Lee et al. (2006) have suggested that the Keeling intercept is an ambiguous quantity that should not be used to interpret the isotope composition of ET. In there analysis, they demonstrated that the variation in the isotope composition of water vapor at short timescales (hourly) was strongly controlled by airmass advection. In addition, it is well-established that the concentration footprint of a scalar is considerably larger than that of its flux (Kljun et al., 2004). Therefore, Keeling mixing lines derived from single point concentration measurement may be associated with a source footprint that is less representative of the flux depending on land surface heterogeneity (Griffis et al., 2007).

Micrometeorological applications place considerable demand on instrument performance and isotope applications require careful consideration of sample system design because of the potential to influence isotope fractionation. Although it is not the goal of this review article to suggest a standardized approach to making isotope flux measurements, a few key issues are highlighted. The ideal isotope sensor, capable of remote eddy covariance flux measurements, would have a system response time better than 0.2 s and a corresponding precision better than 0.5‰. The sensor calibration should be stable over relatively long averaging intervals (30–60 min). For remote field applications it would be ideal if the sensor did not require cryogens such as liquid nitrogen for cooling the laser or its detectors (Saleska et al., 2006). Further, for aircraft applications the sensor should have minimal sensitivity to vibrations. At the present time, none of the instruments reviewed above, satisfy all of these demands, which continues to inhibit progress and wider application of these techniques. The feasibility of making isotope flux measurements, however, has increased as optical methods have become available with increased frequency response and improved precision. While many of the optical isotope analyzers reviewed above (Table 2) have measurement frequencies ranging from 0.3 Hz to 20 Hz, this should not be mistaken as the system response time. The system response time will also be influenced by the sample cell volume, sample tubing volume, pressure, flow rate, electronic signal filtering/processing, etc. Therefore, although the measurement frequency may be adequate for an application such as eddy covariance, the air sampling scheme and other system characteristics need to be optimized to maintain turbulent flow (Reynolds number greater than 2300) so that the system captures the dominant frequencies contributing to the flux.

Isotope applications are also susceptible to air sample tubing effects. Factors including equilibration time, attenuation, kinetic fractionation, and sample memory effects must be considered in the design of such systems. These issues are especially important for water vapor applications because of sorption and desorption on the surfaces of tubing. Sturm and Knohl (2009) investigated the influence of Synflex and Teflon tubing types on water vapor isotope measurements. They concluded that Synflex had a slower equilibration time and an apparent kinetic fractionation effect for deuterium, presumably because this isotopologue has stronger sorption/desorption properties. Griffis et al. (2010) found that natural coloured high density polyethylene (HDPE) tubing performed equally or better than Teflon tubing. In their water vapor eddy covariance experiment, kinetic fractionation and other adverse tubing effects were minimized by ensuring the sample tubing was heated and that turbulent flow was maintained through the system. It should be emphasized that equilibration time, attenuation, kinetic fractionation, and memory effects are expected to be humidity dependent (Massman and Ibrom, 2008; Fratini et al., 2012) and will also vary depending on the size of concentration step change among sample inlets and calibration standards. With these measurement issues and limitations in mind, recent experiments that report isotope fluxes based on flux–gradient and eddy covariance theory are reviewed below.

Yakir and Wang (1996) were the first to combine the flux–gradient approach with isotope observations of ^{13}C-CO_2, ^{18}O-CO_2, and ^{18}O-H_2O to partition net ecosystem CO_2 exchange into its gross components for agricultural crops. In their study they used flask sampling and IRMS analysis and the Keeling plot (derived as a function of height not time) approach to determine the isotope composition of the net CO_2 flux and demonstrated reasonable success for a short campaign of a few days. More recently, flux–gradient and optical isotope methods have been applied over agricultural surfaces, forests, and below a forest canopy (Griffis et al., 2005b; Lee et al., 2007; Santos et al., 2012). In each of these studies a TDLAS approach (TGA100A, Campbell Scientific Inc.) was used to quantify the isotopologue gradient (^{13}C-CO_2, ^{12}C-CO_2, ^{18}O-CO_2, ^{18}O-H_2O, H_2O) in order to calculate the isotope composition of the net flux. In this methodology, the eddy diffusivity for the major and minor isotopes are assumed identical so that the calculation simplifies to a ratio of the isotope gradients (the flux ratio approach) (Griffis et al., 2004),

$$\delta_F = \left(\frac{\overline{d^H C}/\overline{d^L C}}{R_{\mathrm{std}}} - 1 \right) \tag{3}$$

where δ_F is the isotope composition of the net flux, the overbar indicates the averaging period, superscripts H and L represent the heavy (minor) and light (major) isotopes, respectively for the scalar concentration (C) of interest. In our own work over agricultural ecosystems we determined that the flux ratio method worked reasonably well when the CO_2 concentration gradient was greater than about 3.5 μmol mol^{-1} m^{-1}, yielding an uncertainty in the δ^{13}-CO_2 flux ratio of about 0.8‰. Drewitt et al. (2009) and Glenn et al. (2011) used a similar methodology over agricultural surfaces, but selected a laser with a stronger set of absorption lines for ^{13}C-CO_2 and ^{12}C-CO_2, thereby, improving the signal to noise ratio in the concentration measurements. In their studies they noted that the uncertainty in the flux ratio was typically 2‰ when the CO_2 gradient was less than 1 μmol mol^{-1} m^{-1} and improved to about 0.7‰ for a gradient of 3.5 μmol mol^{-1} m^{-1}. Based on these two recent studies we can conclude that selecting stronger absorption lines does not guarantee a substantive increase in the flux ratio precision, presumably because the inherent meteorological (random) noise is the main limiting factor. Lee et al. (2007) simulated typical water vapor mixing ratio and isotope gradients in the laboratory using a Rayleigh distillation technique in order to quantify the typical flux ratio precision. For daytime conditions above a forest, their TDLAS and gradient sampling scheme yielded a flux ratio precision of about 1.4‰ for ^{18}O-H_2O. The magnitude of these errors become particularly important when the goal is to partition F_N or ET based on isotope differences (disequilibrium) among the gross flux components (soil evaporation, transpiration, respiration, photosynthesis). These issues are discussed further in the flux partitioning section.

Santos et al. (2012) recently applied the flux ratio methodology below a mixed deciduous forest canopy at the Environment Canada Research Station in Borden, Ontario, Canada in order to estimate the oxygen and carbon isotope composition of the soil CO_2 efflux. Under these conditions, flux–gradient measurements are susceptible to counter-gradient transport and the near-field effect acts to decouple the vertical gradient (dc/dz) from the local vertical flux density (Corrsin, 1974; Denmead and Bradley, 1985; Simpson, 1998; Lee, 2003). While the flux–gradient approach typically underestimates the flux magnitude under these conditions, the experimental data presented by Santos et al. (2012) indicate that the flux ratio can be resolved reasonably well in this environment. Their flux ratio results were also supported with an independent inverse Lagrangian approach. Further, their work demonstrated that greater data retention (95% of the observations) was possible when using the flux ratio method. In comparison, the Keeling method resulted in 27% data retention because of inadequate concentration range and relatively large uncertainties in the estimate of the regression intercept. This work represents an important step because below canopy fluxes are needed to gain new information regarding the behavior of soil respiration, its partitioning, and changes in its carbon and oxygen isotope composition that are driven by different environmental factors. While chamber systems are increasingly being coupled with optical isotope systems to address these issues, chamber data have come into question because of a number of chamber artifacts that make their interpretation difficult (discussed later). Ideally, below canopy eddy

covariance (Blanken et al., 1998) isotope flux measurements could be used to address these important issues.

Eddy covariance isotope flux measurements have been pursued for a number of reasons. The theory is based on first principles and has few underlying assumptions when compared to other approaches such as flux–gradient, relaxed eddy accumulation, or Monin–Obukhov similarity theory. Ideally, the eddy covariance approach could be used in situations where the flux–gradient is known to be less reliable (i.e. below forest canopies or above tall vegetation) or not possible (i.e. aircraft). The pioneering work of Bowling et al. (2003a) used a conditional sampling approach (hyperbolic relaxed eddy accumulation) and flask air collection and IRMS to measure the isotope composition of NEE. The main limitation in their study was the need to collect, transport, and analyze a significant number of flasks in order to resolve the fluxes over the course of a few days. With advances in fast response analyzers it has become possible to measure the isotopic fluxes directly using the eddy covariance approach (Griffis et al., 2008, 2010; Sturm et al., 2012). Here the flux ratio can be derived from,

$$F^x = \overline{\rho}_a \overline{w' \chi^x_{s'}} + S^x = \overline{\rho}_a \int C^x_{W\chi_s}(f)df + S^x \quad (4)$$

where, $\overline{\rho}_a$ is the molar density of dry air, w is the vertical wind velocity, χ_s is the total molar mixing ratio for a given scalar (i.e. H_2O or CO_2), the primes indicate the differences between instantaneous and mean values and the overbar indicates an averaging operation (i.e. 30-min integration period). Here $\overline{w'\chi_{s'}}$ is the covariance of w and χ_s and is equivalent to the co-spectral density of the fluctuations in vertical wind velocity and the scalar mol mixing ratio ($C_{W\chi_s}$), where f is the frequency. The storage term (S) is defined as the rate of change in the scalar between the ground and the eddy covariance measurement height. The superscript x indicates one of the isotopologues.

The isotope composition of the flux can be determined from the flux ratio,

$$\delta_F = \left(\frac{F^H/F^L}{R_{\text{std}}} - 1 \right) \quad (5)$$

with the isotope ratio reported relative to R_{std}. These high frequency measurements also provide an opportunity to explore the cospectral flux ratio as a function of eddy frequency. This technique may lead to new process information regarding the source origin of the scalar in turbulent transport and boundary layer flows,

$$\delta_F(f) = \left(\frac{C^H_{W\chi_s}(f)/C^L_{W\chi_s}(f)}{R_{\text{std}}} - 1 \right) \quad (6)$$

In the case for CO_2, the first experiments were conducted over agriculture (soybean) (Griffis et al., 2008) and forest (Sturm et al., 2012). Griffis et al. (2008) demonstrated that the diel patterns of the ^{13}C-CO_2 and ^{18}O-CO_2 isofluxes were less noisy than for gradient measurements and revealed pronounced diel patterns, which could be used to assess the extent of isotope disequilibrium between daytime and nighttime fluxes. The relative uncertainty in the ^{13}C-CO_2 isoflux was about 30%, larger than the noise in traditional eddy covariance CO_2 flux measurements (Morgenstern et al., 2004). The flux ratios were well behaved when the total CO_2 flux was greater than about 4 μmol m^{-2} s^{-1}. At low flux values (near zero) the flux ratio variability increased and by definition is undefined as the flux tends to zero. An important point to note is that if the one-way fluxes differ in sign, then the flux ratio may not fall within the range of the isotope ratios of the individual fluxes (end-members) (Miller et al., 2003). Thus, there can be large variability in the isotope composition at low flux values that is independent of the instrument noise.

Sturm et al. (2012) have made the first carbon isotope flux measurements above a mixed deciduous forest in Lageren, Switzerland using a combination of eddy covariance and quantum cascade laser absorption spectrometer (QCLAS) technique. Their 4-week field experiment demonstrated that the precision of the approach was not sufficient to resolve the diel variation in ^{13}C-CO_2 discrimination, but were able to detect changes in ^{18}O-CO_2 discrimination that occurred following precipitation events. The application of their methodology above a mature forest presents a number of challenges. The fluxes are relatively small compared to over agriculture and the extent of isotope disequilibrium for ^{13}C-CO_2 is expected to be small (probably less than 1‰ in this case) and, therefore, difficult to resolve by any methodological approach. In their analyses, they concluded that the instrument noise accounted for approximately 10‰ uncertainty in the half-hourly flux ratio calculations and that the inherent meteorological noise contributed a similar amount of uncertainty to the flux ratio. Therefore, they suggest that improvements in the instrumentation (i.e. better temperature stability of the QCLAS) would result in limited improvements in the flux ratio resolution. However, when their data are plotted in the form a linear regression flux ratio plot (Griffis et al., 2007) the discrimination values are better behaved and show considerably less noise. Thus, one potential way forward is to make use of this data analysis technique to capture daily or weekly snap-shots of discrimination, which can be mapped directly to flux footprint climatologies.

Fig. 3 provides examples of flux ratio plots for CO_2 and water vapor measured over soybean and corn systems, respectively at the Rosemount Research and Outreach Center at the University of Minnesota. These daily snapshots of the flux ratios indicate that this tool could provide useful insights regarding the short-term temporal changes in ecosystem discrimination that are driven by variations in hydrometeorological and phenological conditions.

In the case for water vapor, the first eddy covariance flux measurements were conducted over a corn canopy (Griffis et al., 2010). The observed signal to noise ratio was significantly improved compared to our original CO_2 work over soybeans. Strong diel patterns of the isotope composition of evapotranspiration were observed and compared to estimates based on the Craig–Gordon model (Craig and Gordon, 1965). Excellent agreement was observed during the late afternoon when steady-state conditions were approached. Further, non-steady state estimates of canopy-scale leaf water enrichment were derived from these flux measurements and were shown to track individual leaf water values reasonably well so that ^{18}O-CO_2 discrimination could be predicted (Griffis et al., 2011). While the above approaches show promise, an important question remains regarding the extent to which flux-based approaches can be improved. From the literature reviewed above, it appears that further improvements in laser technology (more precise measurement at high frequencies) may lead to relatively small gains in performance. Given that digital filtering improves the TDLAS isotope concentration measurement precision, but does little to improve the flux ratio measurement highlights this fact (Griffis et al., 2008). The major source of uncertainty in flux ratio measurements stem from the inherent random noise in meteorological transport processes. Error propagation in the isotope fluxes based on flux–gradient and eddy covariance techniques generally range from 20 to 30% (Griffis et al., 2008). Given this inherent noise, the majority of the above studies have recommended the use of ensemble averaging over periods of days to months to help improve the signal to noise ratio. Good et al. (2012) have recently drawn similar conclusions and demonstrated that the random error propagation is expected to be larger for the eddy covariance approach compared to the traditional Keeling method. However, their analyses did not consider the important systematic errors associated with the Keeling method as discussed above. Eddy covariance and flux–gradient isotope measurements could

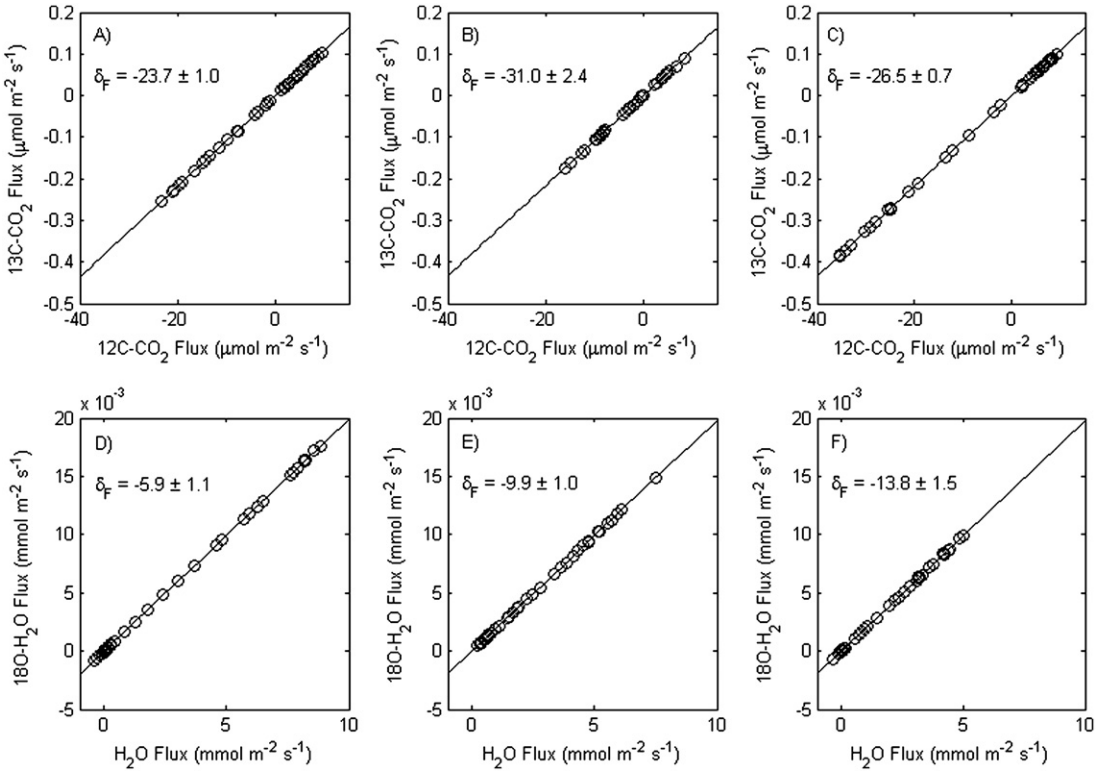

Fig. 3. Examples of flux ratio plots for CO_2 and water vapor based on the eddy covariance approach. The top panels show daily eddy covariance carbon isotope flux ratio estimates above a soybean canopy for (A) DOY 205, 2006; (B) DOY 213, 2006 and (C) DOY 217, 2006. The bottom panels show daily eddy covariance water vapor isotope flux ratio estimates above corn canopy for (D) DOY 173, 2009; (E) DOY 179, 2009 and (F) DOY 213, 2009. The regressions shown in each figure are based on the geometric regression. The slope of each linear plot was converted to delta notation using Eq. (5).

be optimized to improve the signal to noise performance within certain limitations imposed by site characteristics and theoretical considerations. For example, placement of sensors closer to the sink/source could improve the signal to noise ratio, however, measurements made within the roughness sub-layer may be less representative because of the smaller source footprint and effects of wake elements. Increasing the separation distance between sample inlets for flux–gradient measurements could also improve the signal to noise performance, however, adequate fetch and surface homogeneity often limit such approaches. Finally, given that the majority of commercially available optical isotope sensors have system response times that are inadequate for the eddy covariance application, their application to obtaining relatively high-frequency canopy profiles in conjunction with an inverse Lagrangian approach may be particular powerful for partitioning CO_2 and water vapor fluxes. The recent work of Santos et al. (2012) illustrates the potential power of this methodology.

5. Applications of micrometeorological and stable isotope techniques

In this section I examine how isotope techniques have been applied under field conditions to study a number of relevant canopy-scale problems in land-atmosphere exchange. In particular, the partitioning of net fluxes into the gross components, biophysical controls on ecosystem respiration and canopy-scale leaf water enrichment, and the coupled carbon–water isotope budgets are examined.

5.1. Partitioning net ecosystem CO_2 exchange

One of the early motivations for combining stable isotope and micrometeorological techniques was to partition the net ecosystem CO_2 exchange (F_N) into its gross components to better understand how environmental factors influence ecosystem respiration and photosynthesis separately at relatively large spatial scales (ecosystem to region) (Yakir and Wang, 1996). The theory for isotope flux partitioning is developed more fully later, but for now, note that this approach is based on an assumption that there exists a difference (D, disequilibrium) between the isotope composition of photosynthesis (δ_A) and ecosystem respiration (δ_R) (i.e. $D = \delta_A - \delta_R$). Carbon isotope disequilibrium can be linked to historical changes in the isotope composition of the atmosphere and the relatively long residence time of soil organic matter (Trumbore, 2006) and is known as the Seuss effect (Francey et al., 1999). Preindustrial atmospheric δ^{13}C-CO_2 was approximately −6.5‰ and has been declining steadily to current values of −8.2‰ as a consequence of burning ^{13}C-depleted fossil fuel sources. The "heavier" carbon signal was slowly recorded into biomass and soil organic matter *via* photosynthesis. Ecosystem respiration, therefore, represents a mixture of old/new carbon sources so that its isotope ratio should differ from recent photosynthates. Therefore, in global inverse studies that make use of carbon isotope information, the expectation has been that $D < 0$ (Fung et al., 1997; Randerson et al., 2002). However, the extent and sign of this disequilibrium can vary dynamically for different ecosystems, depending on carbon turnover rates, disturbance history and climate, and ultimately represents the minimum flux ratio detection limit that is required in order to pursue flux partitioning successfully.

In the first ecosystem scale isotope partitioning study of F_N, Yakir and Wang (1996) used a micrometeorological aerodynamic approach with air flask sampling and isotope ratio analysis using IRMS. Their results were very promising and showed that midday F_N could be partitioned into the gross components for wheat, cotton, and corn using both the ^{13}C-CO_2 and ^{18}O-CO_2 isotope tracer approach. Their partitioning was performed independently using

Table 3
Isotope (^{13}C-CO_2 and ^{18}O-CO_2) disequilibrium observed under field conditions.

Study	Ecosystem	^{13}C-CO_2 disequilibrium	^{18}O-CO_2 disequilibrium	Comments
Yakir and Wang (1996)	Wheat, cotton, corn in central Israel	<2	10.2–15.3	^{18}O-CO_2 of photosynthesis assumes full isotope equilibration with bulk leaf water
Bowling et al. (2001)	Deciduous forest, Tennessee, USA	<1	–	First study to solve for canopy-scale isotope composition of photosynthesis based on big leaf model and isotope partitioning theory
Lai et al. (2003)	C_3/C_4 prairie, Kansas, USA	0–14	–	Carbon isotope disequilibrium values highly dynamic due to C_3/C_4 phenology. Disequilibrium values approached 0 during periods of drought
Ogée et al. (2003, 2004)	Pine forest, France	<3	12.0–17.0	Maximum carbon isotope disequilibrium was observed at midday
Zhang et al. (2006)	Corn following soybean, Minnesota, USA	1–9	–	Maximum carbon isotope disequilibrium was observed in spring/fall suggesting strong mid-growing season coupling between photosynthesis and respiration
Aranibar et al. (2006)	Old growth Ponderosa Pine, Oregon, USA	<2	–	Measured values of the carbon isotope ratio of photosynthesis ranged between −27.0 and −24.5‰. Measured values of the carbon isotope ratio of respiration ranged between −26 and −25‰ (data obtained from McDowell et al. (2004))
Zobitz et al. (2008)	Sub-alpine forest, Niwot Ridge, Colorado, USA	<2	–	Demonstrated that carbon isotope disequilibrium ranged between positive and negative values of about 2
Billmark and Griffis (2009)	Soybean following corn, Minnesota, USA	2–6	–	Stronger carbon isotope disequilibrium for soybean than corn systems
Wingate et al. (2010a)	Pine forest, France	–	2.0–10.0	Large day to day and seasonal variation in oxygen isotope disequilibrium. Typical daytime values around 10‰. Minimum oxygen isotope disequilibrium observed following precipitation
Griffis et al. (2011)	Corn following soybean, Minnesota, USA	–	0.3–17.1	Minimum oxygen isotope disequilibrium observed following precipitation; median summertime value of 7.8‰
Santos et al. (in prep)	Deciduous forest, Ontario, Canada	–	0–12.0	Highly variable through the growing season and very sensitive to canopy CO_2 hydration efficiency

Isotope disequilibrium is defined here as the absolute difference in isotope composition between the photosynthetic and non-foliar respiratory fluxes, $D = |\delta_A - \delta_R|$ for both ^{13}C-CO_2 and ^{18}O-CO_2, and is expressed in per mil.

each tracer and yielded similar gross flux estimates. The isotope disequilibrium for their ^{13}C-CO_2 observations was relatively small (<2‰), but significantly larger (>10‰) for their ^{18}O-CO_2 approach (Table 3). One important limitation to their approach was that the key isotope end members for photosynthesis and respiration were derived from the IRMS analysis of individual plant leaf and soil organic matter samples. Therefore, the methodology did not account for the short-term temporal variability in these end members, nor did it represent a true canopy-scale estimate.

Bowling et al. (2001) advanced this original work and made a number of important contributions in terms of the theoretical and technical approach. For review, the basic equations of the isotope partitioning theory are presented below for a C_3 photosynthetic pathway,

$$F_N = F_A + F_R \tag{7}$$

$$F_N\delta_N = F_A(\delta_a - \Delta) + F_R\delta_R \tag{8}$$

$$\Delta = a + (b - a)\frac{C_c}{C_a} \tag{9}$$

$$-F_A = g_c(C_a - C_c) \tag{10}$$

where F_A and F_R are net photosynthetic assimilation and non-foliar ecosystem respiration, respectively. δ_N, Δ, and δ_R represent the isotope composition of F_N, canopy-scale photosynthetic discrimination, and the isotope composition of F_R, respectively. δ_a, a, and b are the isotope composition of CO_2 in the surface layer, kinetic fractionation associated with CO_2 diffusing into the stomata, and enzymatic fractionation associated with ribulose 1,5 bisphosphate carboxylase/oxygenase (rubisco) carboxylation, respectively. Values of a and b are typically 4.4‰ and 29‰, respectively (Farquhar et al., 1989). g_c, C_a, and C_c are the canopy-scale conductance to CO_2, surface layer CO_2 concentration, and CO_2 concentration at the chloroplast (sites of carboxylation), respectively. Bowling et al. (2001) showed that this set of equations yielded a quadratic solution with only one biophysically reasonable value.

A major challenge to implementing this theory was the measurement of δ_N and δ_R on a near-continuous basis. Optical isotope techniques were not available at this time. Here, Bowling et al. (2001) developed a novel technique to approximate the ^{13}C-CO_2 eddy flux. In this approach, ^{13}C-CO_2 fluctuations were essentially modeled using linear regression analysis of flask air samples that were analyzed for their total CO_2 concentration and δ^{13}C-CO_2 content at timescales ranging from seconds to hours. These regression models were then used to propagate ^{13}C-CO_2 from traditional fast (10 Hz) measurements of CO_2 using an infrared gas analyzer. Further, δ_R was quantified on a near-continuous basis using the nighttime Keeling plot approach. This new theory and measurement approach was applied over a temperate deciduous forest (Walker Branch Watershed, Tennessee, USA). Their analyses indicated that the use of the ^{13}C-CO_2 tracer provided additional information that allowed useful flux partitioning. However, one of the main limitations identified was that the F_N partitioning was highly sensitive to the canopy-scale CO_2 conductance and uncertainties related to the Penman–Monteith (PM) big leaf approach. Because the isotope disequilibrium for this forest was relatively small (<1‰), the gross flux estimates were relatively noisy compared to traditional approaches.

Ogée et al. (2003) pursued a similar partitioning approach outlined above for a pine forest near Bordeaux France (over a 22-day period), but used the multi-layer model (MuSICA) to estimate the bulk canopy conductance to CO_2. Their motivation was to provide an estimate of g_c that accounted for the problems of

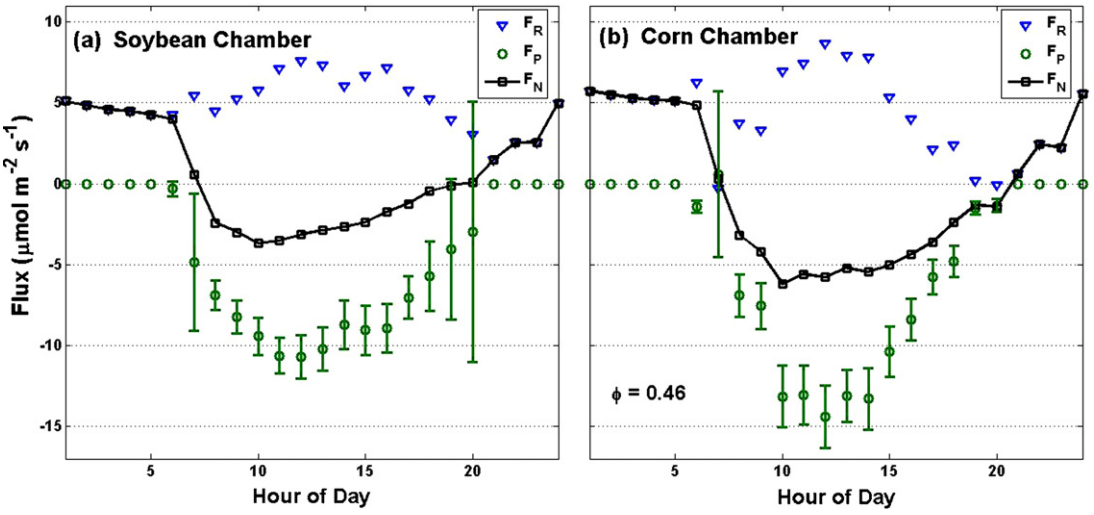

Fig. 4. Diurnal composite of net ecosystem CO_2 exchange (F_N, black squares) partitioned into respiration (F_R, blue triangles) and photosynthesis (F_P, green circles) from the corn and soybean chambers. Ensemble averages were created from the last 15 days of the experiment during peak growth. Error bars represent the maximum probable error propagation (Fassbinder et al., 2012a). Reproduced with permission from the author. (For interpretation of the references to color in this figure legend, the reader is referred to the web version of the article.)

non-linear response through the canopy, soil evaporation contamination, and the lack of energy balance closure observed in field measurements. They observed only a small bias in g_c between the PM approach and their model approach, with PM values slightly lower than MuSICA. This was attributed to the fact that their PM approach was influenced by the lack of energy balance closure. More importantly, they demonstrated that accounting for mesophyll conductance improved their partitioning results. The isotope partitioning methodology worked best near midday when the fluxes were large and the isotope disequilibrium approached its maximum value of about 3‰. In fact, Ogée et al. (2003) showed that strategic sampling during key parts of the diel cycle could be used to pursue the isotope partitioning in a more time/cost efficient manner. Overall, the partitioning results were relatively noisy, but the ensemble diel patterns were in close agreement (within 15–20%) of the simulated values.

Zhang et al. (2006) were the first to use continuous measurement of ^{13}C-CO_2 using TDLAS, and the flux–gradient approach to partition F_N over a C_4 (corn) ecosystem. Their expectation was that near-continuous measurement of the ^{13}C-CO_2 flux and elimination of the Keeling method would significantly improve the reliability of the isotope flux partitioning result. Their analyses and results showed that resolving δ_N (isotope composition of F_N) was difficult because of the relatively small gradient observed above the canopy, despite relatively large fluxes in an agricultural system. Further, they found that the isotope partitioning approach was particularly problematic during the peak growing season when the carbon isotope disequilibrium became relatively small. In fact, it was relatively surprising that an agricultural ecosystem growing in a corn–soybean rotation would approach near equilibrium by mid growing season. It further illustrates the strong dependence of respiration on recent photosynthates (Griffis et al., 2005b; Rochette and Flanagan, 1999). The small disequilibrium (on the order of 1‰ at mid growing season) places much higher demand on resolving the ^{13}C-CO_2 flux. However, it should also be noted that partitioning F_N in a C_4 ecosystem is complicated by the need to estimate the bundle sheath leakage parameter making the partitioning approach somewhat more difficult than for C_3 ecosystems because there are no direct measurements of this additional variable.

Zobitz et al. (2007) partitioned F_N at the Niwot Ridge subalpine forest using a combination of high frequency carbon isotope TDLAS measurements and a Bayesian optimization approach. This work advanced the earlier isotope-Bayesian approach introduced by Ogée et al. (2004). Here, Zobitz et al. (2007) made use of an unprecedented high density isotope dataset and computed δ_N for each half-hourly period during the growing season. Their analyses demonstrated that these new data reduced the prior uncertainty of the Bayesian parameters. However, further analysis indicated that Bayesian-derived F_A and F_R showed dependence on the choice of their prior values. Thus, this indicated that the information contained in the data was not sufficient to independently partition F_N. Again, the isotope disequilibrium was relatively small for this forest and ranged from only −2‰ in early morning and early evening to +2‰ at midday. The relatively small disequilibrium probably explains the dependence of the Bayesian-derived values of F_A and F_R on their prior values. Zobitz et al. (2007) identified four main factors that may have limited their carbon isotope partitioning methodology including: (1) small isotope disequilibrium; (2) the need for a direct measurement of the ^{13}C-CO_2 eddy flux; (3) scaling of leaf-scale biophysical processes (i.e. discrimination, conductance) to the canopy; and (4) errors in estimating the canopy conductance to CO_2.

Billmark and Griffis (2009) compared the flux–gradient approach with the first eddy covariance measurements of ^{13}C-CO_2 exchange above a soybean canopy to partition F_N. They demonstrated reasonable success using both methods and showed that the partitioning result was improved significantly compared to their earlier work over a C_4 corn canopy. An important finding in their study was that the isotope partitioning methodology was less reliable at midday using the flux–gradient approach. During these periods F_A was not significantly different than F_N. This midday isotope partitioning anomaly was attributed to the difficulty of resolving midday isotope gradients above a canopy when the atmosphere is well mixed. When compared to the eddy covariance approach this midday anomaly disappeared and F_A values were significantly larger and more symmetric about F_N. Here, the isotope disequilibrium over the diel period ranged from about 2 to 6‰. These favorable partitioning results can largely be attributed to this relatively large disequilibrium.

Given the inherent complexity in ecosystem-scale studies we recently performed a growth chamber experiment to re-examine the isotope flux partitioning methodology under simplified and controlled environmental conditions inside a greenhouse (Fassbinder et al., 2012a). Using a combination of small automated

growth chambers and TDLAS, we measured the isotope composition of F_N for small plant communities (corn and soybean) and measured the isotope composition of soil respiration directly from chambers containing native soil without vegetation. In addition, this simple approach eliminated the need for PM measurements and provided a direct estimate of soil evaporation, presumably improving our estimate of CO_2 conductance. Further, with improved signal to noise isotope flux measurements, and controlled environmental conditions, an in-depth analysis of isotope flux partitioning theory for both C_3 and C_4 photosynthetic pathways was possible. The results are presented here in Fig. 4. Fassbinder et al. (2012a) confirmed the very high sensitivity of the carbon isotope flux partitioning approach to CO_2 conductance. Further, their work demonstrated that the short-term variability in δ_R had a very important influence on partitioning in both C_3 and C_4 systems, with C_4 systems showing greater sensitivity. The variability in δ_R was significant over the diel cycle and was especially pronounced following post-illumination. Overall, the isotope partitioning approach was improved by accounting for the variability in δ_R. Finally, under these ideal conditions we compared the isotope partitioned fluxes with traditional regression-based approaches and concluded there were systematic differences in the pattern of photosynthesis and respiration related to each approach. We suggested that the lack of sensitivity of autotrophic respiration to variations in temperature was an important factor.

From the literature reviewed above it can be concluded that the ^{13}C-CO_2 isotope partitioning approach is strongly limited by the tradeoff in measurement precision of the isotope fluxes and the extent of disequilibrium between photosynthesis and respiration. In the majority of the studies reviewed, the ^{13}C-CO_2 disequilibrium was typically less than 3‰, thereby, placing high demands on the measurement precision. Further, when examining the isotope partitioned fluxes in comparison to traditional methods (i.e. nighttime temperature-based regression models) we can observe systematic differences in their patterns, with the isotope-partitioned fluxes being symmetric about canopy conductance to CO_2, while the temperature-based approaches are skewed toward the warmer late afternoon temperatures. These patterns deserve further investigation as they may represent a potential bias in current land surface models. Finally, representing the isotope composition of ecosystem respiration in partitioning studies has largely been oversimplified. Accounting for its short-term variability has potential to improve the isotope-based partitioning results.

5.2. Temporal variation in the isotope composition of ecosystem respiration

While the processes influencing photosynthesis and photosynthetic fractionation are relatively well known (Farquhar, 1983; Farquhar et al., 1989, 2001), there is significantly less information and theoretical understanding of ecosystem respiration and fractionation effects associated with respiration processes (Bowling et al., 2008; Wingate et al., 2010b; Flanagan et al., 2012). In the above flux partitioning studies it was assumed that any isotope fractionation associated with respiration was negligible (Lin and Ehleringer, 1997) and that respiration from various ecosystem components was conservative so that nighttime values could be extrapolated to the daytime (Bowling et al., 2001; Ogée et al., 2003; Zhang et al., 2006; Zobitz et al., 2007). Past studies spent considerable effort trying to quantify the isotope composition of ecosystem respiration in order to infer information regarding ecosystem photosynthetic discrimination (assuming full equilibration) (Bowling et al., 2003a; Ponton et al., 2006; Buchmann et al., 1998). More recent studies have attempted to quantify the links between photosynthetic discrimination and downstream changes in the isotope composition of respiration components. The classic work of Högberg et al. (2001) showed that there is a direct link between photosynthetic assimilation and soil respiration. In their study they observed a 2–4 day lag between changes in photosynthetic activity and its influence on soil respiration. Bowling et al. (2003a) showed that variations in the isotope composition of ecosystem respiration could be linked to changes in atmospheric vapor pressure deficit and its influence on stomatal activity and photosynthetic fractionation. Understanding these links is required in order to improve our biophysical description of carbon turnover in ecosystems and for representing respiration processes in land surface schemes.

It is now appreciated that post-photosynthetic isotope fractionation occurs resulting in an apparent fractionation of ecosystem respiration (Duranceau et al., 1999; Ghashghaie et al., 2001; Tcherkez et al., 2003; Hobbie and Werner, 2004; Xu and Baldocchi, 2004; Badeck et al., 2005; Gessler et al., 2007; Bathellier et al., 2008). Isotope fractionation downstream of primary photosynthetic carboxylation, either during assimilate transport or through compartmentalization prior to transport, results in differences in the isotope composition of metabolites and in intramolecular distribution of ^{13}C and ^{12}C from fragmentation of the substrate molecule (Tcherkez et al., 2003, 2004). For example, researchers have observed that dark respiration in C_3 leaves is significantly enriched relative to plant sucrose, the respiration substrate (Duranceau et al., 1999, 2001; Ghashghaie et al., 2001; Tcherkez et al., 2003; Bathellier et al., 2008). Further, Klumpp et al. (2005), Badeck et al. (2005), and Bathellier et al. (2008) have shown that root-respired CO_2 from herbaceous species is relatively depleted in ^{13}C compared to the substrate. Here the underlying mechanism is CO_2 release from the pentose phosphate pathway (PPP) where carbon from the C-1 position in glucose is relatively depleted. Klumpp et al. (2005) demonstrated, through a mass balance approach, that fractionation associated with dark respiration in leaves was nearly balanced by the fractionation in root respiration, such that the overall net fractionation related to plant respiration was relatively small (≈0.7‰).

Rapid changes in the isotope composition of respiration have been linked to post-illumination processes at the leaf, plant, and ecosystem scales (Tcherkez et al., 2003; Gessler et al., 2009; Barbour et al., 2011; Fassbinder et al., 2012a,b). It appears that the timescale of the post-illumination response ranges from minutes to as much as a few hours and that the magnitude of the change in the isotope composition of respiration may be directly related to cumulative daytime CO_2 uptake (Barbour et al., 2011). These underlying mechanisms are becoming better understood. The ^{13}C-enriched CO_2 produced in the dark has been termed Light-Enhanced-Dark-Respiration (LEDR). Gessler et al. (2009) used an isotope mass balance technique to demonstrate, under controlled laboratory conditions, that the source for LEDR enrichment was naturally occurring ^{13}C-enriched malate decarboxylation in leaves. A progressive ^{13}C depletion of CO_2 evolved from leaves in the dark has been observed to decrease by as much as 10‰. Barbour et al. (2011) used the flux ratio and Keeling plot approach to quantify the LEDR effect at the ecosystem scale in pasture lands of New Zealand. Fig. 5 shows an example of rapid changes in the carbon isotope composition of ecosystem respiration following sunset based on fast optical isotope measurements. They observed a stronger effect following sunny days and provided a simple model to help understand the underlying processes and dynamics. It is interesting to note here that such patterns would be difficult, if not impossible, to observe based on traditional measurement techniques such as flask collection and Keeling plot approaches relying on data collected over the entire nighttime period. Fast optical isotope measurements provide a new capacity to examine these dynamics under a broad range of environmental conditions.

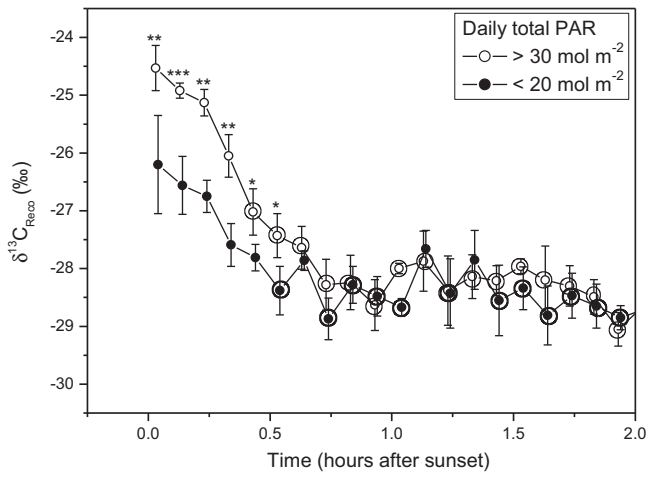

Fig. 5. Rapid changes in the carbon isotope composition of ecosystem respiration following sunset based on fast optical isotope measurements (Barbour et al., 2011). The isotope composition was determined using a Keeling plot and flux ratio approach. Reproduced with permission from the author.

Kodama et al. (2008) examined the temporal variation of δ^{13}C-CO_2 of forest (Scots pine) respiration and its components using a combination of Keeling plot, static chamber and IRMS techniques over a period of about 4 days. In addition, they measured the carbon isotope composition of the water soluble organic matter in foliage needles, twig phloem, and trunk phloem exudate to better understand dynamics of forest respiration and controls on its carbon isotope composition. They observed diel variations (0.6–0.9‰) in the carbon isotope composition of needle phloem with little or no diel variation observed in twig or trunk phloem. The phloem exudate was progressively enriched along the transport pathway from needles to twigs to trunk. The diel variation in respired carbon from the tree boles (4‰) and forest soil (2.7‰) was significant, suggesting an apparent fractionation associated with respiration. As discussed by Kodama et al. (2008), the large diel variation in the carbon isotope composition of bole respiration could be caused by the playoff between glycolysis and the citrate cycle (mitochondrial respiration). The δ^{13}C-CO_2 derived from both processes are expected to differ as a result of fragmentation fractionation (Ghashghaie et al., 2001, 2003; Tcherkez et al., 2003, 2004; Hymus et al., 2005). The CO_2 released by the decarboxylation of pyruvate (glycolysis) comes from the relatively ^{13}C-enriched C-3 and C-4 positions of glucose. The CO_2 released from the citrate cycle decarboxylation originates from the relatively depleted C-1, C-2, C-5, and C-6 positions of glucose. Each of these cycles has different temperature dependencies, with glycolysis being less temperature-dependent than the citrate cycle. Therefore, changes in autotrophic respiration driven by temperature have significant potential to cause variation in the isotope composition of respiration. Finally, they observed a 2‰ variation in the isotope composition of forest soil respiration measured using a static chamber technique. This variation was attributed to the relative contributions of autotrophic and heterotrophic respiration over the diel period.

Wingate et al. (2010b) have provided one of the most comprehensive datasets and systematic analyses regarding the relation between photosynthetic discrimination and the isotope composition of ecosystem respiration components by combining TDLAS and dynamic chambers. Their study was conducted in a maritime pine forest (Bordeaux France) over the 2007 growing season. They observed strong ^{13}C enrichment (3–4‰ relative to the photosynthate) in branch respired CO_2. This enrichment was likely the result of CO_2 generated by the pyruvate dehydrogenase (PDH) complex and the release of carbon from the enriched C-4 position of glucose. Contrary to Kodama et al. (2008), bole respiration was relatively depleted (2–4‰) compared to the photosynthate. Wingate et al. (2010b) hypothesized that refixation of CO_2 by phosphoenol pyruvate carboxylase (PEPC) within the stem was an important underlying mechanism. PEPC fractionates (5.7‰) against ^{13}C and is well known for its role in C_4 photosynthetic fractionation. Further, the synthesis of lignin *via* PPP could also result in a relatively depleted signal since the source of carbon is known to originate from the C-1 position of glucose. Finally, Wingate et al. (2010b) examined the correlation and lag between changes in photosynthetic discrimination and changes in the isotope composition of respiration from forest components. Their analyses revealed broad seasonal coherence, confirming that photosynthetic discrimination influences the substrates that are eventually metabolized. However, at times there appeared to be little or no coherence among signals indicating the importance of carbon allocation processes, downstream isotope mixing of carbon substrates, and fractionation related to the respiration processes.

Recent work by Fassbinder et al. (2012b) provide one of the longest time series of soil carbon isotope flux measurements using a TDLAS and automated chamber system. Their measurements were made in an agricultural ecosystem during the corn phase of a corn–soybean rotation over the majority of the growing season. Their work demonstrated that the mean ensemble diel peak-to-peak variation in the isotope composition of soil respiration was about 2‰, consistent with other values reported in the literature (Maseyk et al., 2009; Werner and Gessler, 2011). However, larger diel variations were observed, ranging up to 10‰ on individual days. The largest diel amplitudes were observed during the early growing season when soil respiration was relatively small and the vegetation was just beginning to emerge. Fassbinder et al. (2012b) hypothesized that cases with exceptionally large diel amplitude could be attributed to the influence of turbulence (non-diffusive transport) and non-steady state conditions on the chamber measurement technique. They demonstrated a strong positive correlation between the carbon isotope composition of soil respiration and friction velocity, providing anecdotal evidence that CO_2 transport from the soil to the chamber was not always dominated by diffusion. Their analyses also demonstrated that these effects were more pronounced during the early growing period when the chambers were directly exposed to wind (i.e. no canopy shelter effect) and when soil water content was relatively low. Interpretation of soil chamber data is, therefore, challenging because it represents a mixture of both the biological and physical processes.

The application of chamber and isotope-based measurements under field conditions has raised numerous questions regarding the interpretation of the isotope signatures. It is well known that chambers impact wind, turbulence, pressure pumping, and non-steady-state diffusion (Livingston and Hutchinson, 1995; Davidson et al., 2002; Jassal et al., 2012). Here, the challenge is to determine the biological and physical factors influencing the isotope composition of the flux (Midwood and Millard, 2011). Risk and Kellman (2008) demonstrated that under non-steady-state conditions the kinetic fractionation was typically less than the theoretical value of 4.4‰. Consequently, under these conditions, the isotope composition of the flux can be significantly depleted relative to the actual CO_2 source. Bowling and Massman (2011) also confirmed that non-steady-state diffusion through a snowpack resulted in a kinetic fractionation that was lower than the theoretical value and an isotope flux that was relatively depleted compared to the source. Hence, in situations where non-diffusive transport takes place, the isotope composition of the flux will be depleted relative to the actual source value. Further, a number of other studies have documented the importance of advection and infiltration of relatively enriched CO_2 air on chamber flux measurements. Midwood and

Millard (2011) found that advection/infiltration had a large influence on the isotope composition of the flux in soils that were dry and relatively porous, especially during periods when respiration rates were relatively small. Kayler et al. (2010) have suggested that advection accounted for about 1‰ of the variation observed in their forest soil respiration data. However, it is expected that the influence of advection could be substantially larger in situations where the chamber measurements are made in non-sheltered areas where direct exposure to wind and turbulence can play a more important role. The data presented by Fassbinder et al. (2012b) indicate that these effects could be as large as a few per mil over bare agricultural soils. It would appear, therefore, that soil chamber isotope data should be interpreted with the aid of a physical model that can be used to describe the non-biological influences in order to place constraints on these separate processes (Risk et al., 2012).

These recent studies confirm that there is significant variation in the isotope composition of respiration derived at the component and ecosystem scale as a result of post-photosynthetic fractionation processes. The combination of optical isotope measurements with chamber and micrometeorological techniques is providing a new capacity to detect fast and short-term variations in the isotope composition of respiration. The link to compound-specific carbon isotope ratio analyses is proving to be a powerful way to help interpret respiration processes that have, until now, been treated as a black box. Such advances are important in order to provide a better biophysical description of respiration processes in land surface models.

5.3. Canopy-scale leaf water ^{18}O enrichment

The oxygen isotope composition of leaf water represents a highly valuable tracer in global change studies. Daytime enrichment of the leaf water is the combined result of kinetic fractionation (i.e. the lighter H_2O isotope diffuses faster than ^{18}O-H_2O or ^{2}H-H_2O) and equilibrium fractionation (i.e. the lighter H_2O molecule has a higher saturation vapor pressure compared to ^{18}O-H_2O or ^{2}H-H_2O) (Craig and Gordon, 1965; Dongmann et al., 1974). Consequently, at midday the isotope composition of the bulk leaf water ($\delta_{L,b}$) can be significantly enriched relative to the source or plant xylem water (δ_x). This leaf water signal is incorporated into plant cellulose making it a powerful tracer in biomarker and paleoclimate studies (Barbour et al., 2007; Helliker and Richter, 2008; Ogée et al., 2009; Kahmen et al., 2011). The oxygen isotope composition of leaf water also represents a critical boundary condition for determining the oxygen isotope composition of photosynthesis (Farquhar et al., 1993; Yakir, 2003) and influences the Dole effect (Dole et al., 1954; Bender et al., 1994; Hoffmann et al., 2004). Further, partitioning evapotranspiration into its components using the isotope mass balance approach requires information regarding the isotope composition of transpiration (Yakir and Wang, 1996; Yepez et al., 2003; Williams et al., 2004; Lee et al., 2007; Wang et al., 2010, 2012).

A considerable amount of research has examined leaf water enrichment at the leaf and plant scales. These investigations have evolved from relatively simple models that assume the leaf is a well-mixed homogeneous pool in steady state (Craig and Gordon, 1965) to the very sophisticated models that account for leaf water isotope heterogeneity and non-steady state conditions (Farquhar and Cernusak, 2005; Ogée et al., 2007). Far fewer studies have attempted to measure the canopy scale leaf water enrichment or attempted to evaluate applicability of these models at the canopy-scale. With the increasing availability and use of optical isotope methods, there have been important advances in quantifying the canopy scale isotope composition of ET and leaf water enrichment (see Table 4 for examples) (Lee et al., 2007; Welp et al., 2008; Griffis et al., 2010; Rambo et al., 2012). These investigations have been motivated by the need for biophysical information that bridges the gap between the plant and canopy scales and the need to represent canopy scale processes within land surface schemes (Riley et al., 2002, 2003; Xiao et al., 2010, 2012). In this section, recent progress in determining the canopy scale leaf water ^{18}O enrichment and its relevance to flux partitioning and carbon cycling is examined.

With increased capacity to measure the isotope composition of water vapor and fluxes at the field scale, it has become possible to evaluate in detail the biophysical processes and models of leaf water enrichment of varying complexity (Craig and Gordon, 1965; Dongmann et al., 1974; Farquhar and Cernusak, 2005) under field conditions (Lee et al., 2007; Welp et al., 2008; Griffis et al., 2011; Xiao et al., 2012). Three key issues have emerged from recent ecosystem scale studies that are related to the behavior/description of leaf water turnover, kinetic fractionation, and the Péclet effect. Each of these issues is described below.

The classic Craig–Gordon (CG) model predicts leaf water enrichment at the sites of evaporation assuming steady-state conditions (i.e. that the isotope composition of the inflow = the outflow) (Craig and Gordon, 1965):

$$\delta_{L,s} = \delta_x + \epsilon_{eq} + \epsilon_k + h(\delta_v - \epsilon_k - \delta_x) \quad (11)$$

where $\delta_{L,s}$ is the isotope composition of leaf water at the site of evaporation and is calculated assuming steady-state conditions, δ_x is the isotope composition of the xylem water, h is the relative humidity expressed at the leaf surface temperature, δ_v is the isotope composition of the vapor, ϵ_{eq} is the temperature-dependent equilibrium fractionation effect, and ϵ_k is the kinetic fractionation factor (both fractionation factors are expressed as deviations from 1). Here, ϵ_k is presented as the leaf-scale resistance-weighted value (Farquhar et al., 1989; Cappa et al., 2003),

$$\epsilon_k = \frac{32r_s + 21r_b}{r_s + r_b} \quad (12)$$

where r_s and r_b are the stomatal and leaf boundary-layer resistances to water vapor transport and the factors 32 and 21 are the corresponding fractionation factors for ^{18}O-H_2O (Cappa et al., 2003). The CG model is relatively easy to implement now that δ_v can be measured near continuously using optical isotope methods. Table 4 provides a number of examples where the CG model has been used in conjunction with optical isotope measurements to estimate the steady or non-steady state isotope composition at the sites of evaporation. In the latter case, δ_x is replaced with the canopy-scale estimate of the isotope composition of transpiration (Welp et al., 2008). It has become well established that the steady-state condition is often violated (Dongmann et al., 1974; Bariac et al., 1989; Flanagan et al., 1991). However, recent studies based on optical isotope techniques have shown that the CG model performs reasonably well for a short duration in the afternoon hours when near steady-state conditions are likely to prevail (Welp et al., 2008; Xiao et al., 2010; Griffis et al., 2010).

Dongmann et al. (1974) adapted the CG model and proposed that the non-steady state behavior could be accounted for by including the leaf water turnover rate, while holding the leaf water content fixed,

$$\delta_{L,b} = \delta^s_{L,b} + (\delta^0_{L,b} - \delta^s_{L,b})e^{-t/\tau} \quad (13)$$

where $\delta^0_{L,b}t$ is the initial isotope composition of the bulk leaf water, t is time and τ is the water turnover rate and can be estimated from,

$$\tau = \frac{Wr_t\alpha_k\alpha_{eq}}{w_i} \quad (14)$$

where W is the canopy water content per unit ground area, w_i is the mole fraction of water vapor in the intercellular space, r_t is the total resistance to water vapor diffusion. Here, the kinetic and equilibrium fractionation factors are given as, $\alpha_k = 1 + \epsilon_k/1000$ and $\alpha_{eq} = 1 + \epsilon_{eq}/1000$.

Table 4
Estimates of canopy-scale ^{18}O-H_2O leaf water enrichment.

Study	Ecosystem	^{18}O-H_2O enrichment at the sites of leaf water evaporation	Methods	Comments
Lai et al. (2006)	Douglas-fir forest, Washington, USA	Late afternoon maximum value of 10‰	Derived from the Dongmann et al. (1974) non-steady state model using field observations; no turbulent kinetic effect included	Turnover time of leaf water set to 11 h showed excellent agreement with bulk leaf water isotope ratios; values assuming steady state were more than 5‰ higher than non-steady state values
Welp et al. (2008)	Soybean, Minnesota, USA	Maximum values of 15‰ observed at midday; mean ensemble midday values of 8‰	Derived from the Craig and Gordon (1965) model using field observations; a non-steady state estimate based on a direct flux estimate of the transpiration isotope ratio; no turbulent kinetic effect included	Estimate based on flux–gradient and TDLAS measurements of the isotope composition of ET; midday values assuming steady-state were 2‰ lower than the non-steady state estimate
Wingate et al. (2010b)	Pine forest, France	Maximum values of 19‰ were observed in late afternoon; diurnal amplitude generally varied between −5 and 15‰	Derived from branch chamber observations of O18-CO_2 photosynthetic flux	Estimate based on dynamic chamber observations of branch-scale photosynthesis using TDLAS measurements. Farquhar and Cernusak (2005) non-steady state model tracked the observations reasonably well over the 13-day measurement period
Griffis et al. (2011)	Corn, Minnesota, USA	Maximum values of 15‰ observed at midday; mean ensemble midday values of 10‰	Derived from the Craig and Gordon (1965) model using field observations; a non-steady state estimate based on a direct flux estimate of the transpiration isotope ratio; turbulent kinetic effect included	Estimate based on eddy covariance and TDLAS measurements of the isotope composition of ET; mean midday values in July–August were 10‰. Steady state estimates were 0.6‰ higher than non-steady state estimates; including the turbulent kinetic effect acted to lower the leaf water enrichment estimate by about 2‰
Xiao et al. (2012)	Wheat, Luanchen, North China Plain, China	Maximum values of 12‰ observed at midday; mean ensemble midday values of 5‰	Derived from the Craig and Gordon (1965) model using field observations; a non-steady state estimate based on a direct flux estimate of the transpiration isotope ratio; turbulent kinetic effect included	Estimate based on eddy covariance and TDLAS measurements of the isotope composition of ET; excellent agreement was observed using the Craig and Gordon (1965) and Dongmann et al. (1974) models at midday
Xiao et al. (2012)	Corn, Luanchen, North China Plain, China	Maximum values of 12‰ observed at midday; mean ensemble midday values of 8‰	Derived from the Craig and Gordon (1965) model using field observations; a non-steady state estimate based on a direct flux estimate of the transpiration isotope ratio; turbulent kinetic effect included	Estimate based on eddy covariance and TDLAS measurements of the isotope composition of ET; the Craig and Gordon (1965) and Dongmann et al. (1974) models overestimate the observed midday leaf water enrichment by approximately 4‰ presumably due to the turnover time of leaf water and the non-steady state effects
Santos et al. (in prep)	Deciduous forest, Ontario, Canada	Maximum values of 17‰ observed at midday; mean daytime (1000–1500) values over the growing season were 3‰	Derived at the canopy scale using Craig and Gordon (1965) steady state model and the non-steady state model of Farquhar and Cernusak (2005)	Ambient water vapor ^{18}O-H_2O ratios were measured using TDLAS and used as input for the models. These canopy scale values are modeled and do not include direct measurement of the canopy scale isotope ratio of transpiration. Steady-state estimates showed much stronger diurnal variability than the non-steady state model. Midday steady state model estimates were in better agreement with the bulk leaf water isotope ratios

Estimate of the isotope composition at the sites of leaf water evaporation reported in per mil using the Vienna Standard Mean Ocean Water (V-SMOW) scale. These values represent a boundary condition for understanding the potential variability and magnitude of ^{18}O-CO_2 photosynthetic discrimination, which depends on the extent of O18 equilibration.

This model approach has proven to be very robust when applied to the ecosystem scale for Douglas-fir forest (Lai et al., 2006), corn (Griffis et al., 2011) and wheat (Xiao et al., 2012). Fig. 6 provides an example of this modeling approach and a comparison to eddy covariance estimates of the canopy scale leaf water enrichment over corn at RROC at the University of Minnesota. In this non-steady state approach, δ_x in equation 11 was replaced with the eddy covariance estimate of the oxygen isotope composition of ET. This figure clearly shows the strong differences observed between the steady-state and non-steady-state assumptions and that the Dongmann model performed extremely well until late afternoon/early evening. We hypothesized that this late afternoon bias was an artifact of using a constant value for total canopy water (W).

In a comprehensive analysis for corn and wheat systems, Xiao et al. (2012) concluded that the rate of leaf water turnover had the most significant influence on non-steady-state behavior and model performance at the canopy scale. Since ET can be measured near-continuously at the ecosystem scale using the eddy covariance approach, determining canopy leaf water turnover requires a robust estimate of the total canopy leaf water. This is a challenging task. To date, this has largely be determined from tedious destructive sampling and laboratory work. While there have been some

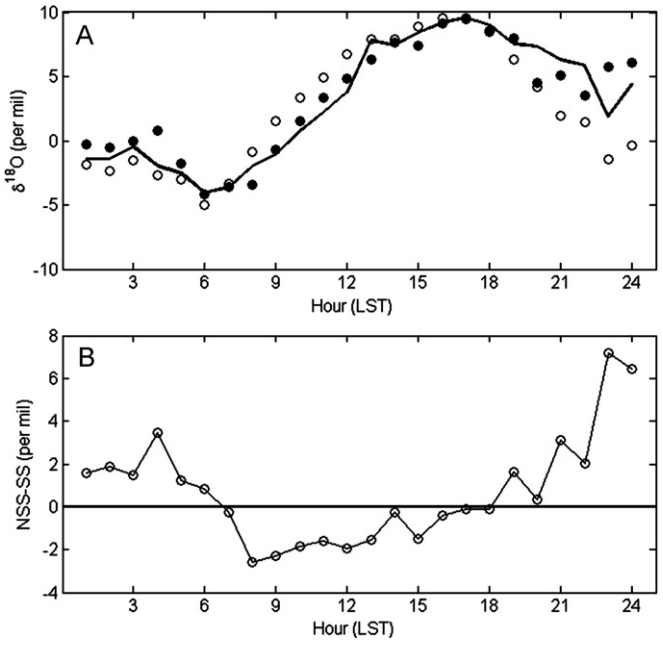

Fig. 6. Estimating the oxygen isotope composition at the sites of leaf evaporation. Ensemble patterns are shown for measurements above a corn canopy during July 2009 at the Rosemount Research and Outreach Center at the University of Minnesota. (A) Steady state ($\delta_{L,s}$, open circle) versus non-steady state ($\delta_{L,e}$, solid black circle) values of the oxygen isotope composition at the sites of leaf evaporation. The steady state values were derived using the Craig–Gordon model and observed stem water isotope ratios. The non-steady state values were derived using the Craig-Gordon model and observed eddy covariance isotope ratios of evapotranspiration. The solid black line indicates the modeled isotope composition at the sites of leaf evaporation based on Dongmann et al. (1974) non-steady state model (see text for details) and (B) the difference between the non-steady state and steady state values over the course of a day (ensemble average).

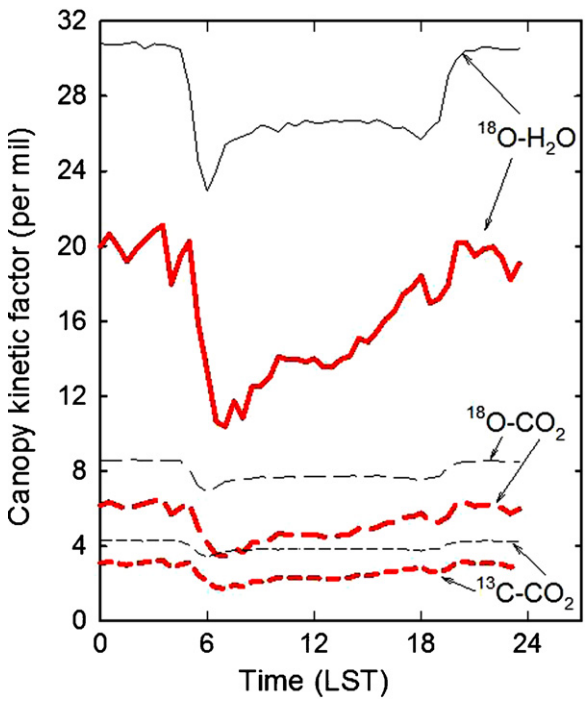

Fig. 7. Diurnal composite of the canopy-scale kinetic fractionation factors (Lee et al., 2009). Thick red lines represent values for a soybean canopy (Rosemount Minnesota) and thin black lines for a mixed deciduous forest (Yale Forest Experiment Station). With the inclusion of turbulent diffusion, the kinetic factors weighted by the gross CO_2 flux are 26.0, 7.6 and 3.8‰ in the forest and 14.1, 4.6, 2.3‰ in the soybean ecosystem, for ^{18}O-H_2O, ^{18}O-CO_2 and ^{13}C-CO_2, respectively. Reproduced with permission from the author.

advances in monitoring leaf water status using satellite techniques (Yilmaz and Jackson, 2008) there is an important need for automated and routine observations at the ecosystem scale. A potential way forward may be the use of technologies such as the Cosmic Ray Soil Moisture Observing System (COSMOS) if it has the sensitivity to track the influence of canopy water from changes in soil water content (http://cosmos.hwr.arizona.edu/).

A second important issue involves the behavior of kinetic fractionation at the canopy scale. Using eddy covariance and flux ratio isotope measurements of water vapor and CO_2 above a soybean canopy, Lee et al. (2009) demonstrated that the kinetic fractionation for water vapor and CO_2 isotopes behaved differently at the canopy scale than at the leaf scale. In their analyses they showed that turbulence acted to enhance kinetic fractionation rather than to diminish it. This effect was found to be most pronounced when canopy resistance was similar or lower than the aerodynamic resistance and was shown to be most significant for ^{18}O-H_2O (Fig. 7). Thus, when micrometeorological measurements are made above the canopy, within the surface layer, the effects of turbulence on kinetic fractionation must be taken into account (Lee et al., 2009),

$$\epsilon_k^c = \frac{32r_c + 21r_b}{r_a + r_c + r_b} \tag{15}$$

where ϵ_k^c is the canopy-scale kinetic fractionation effect for ^{18}O-H_2O, r_c and r_a are the canopy and aerodynamic resistance terms. At the ecosystem scale, the turbulence effect on kinetic fractionation has been shown to have important implications for estimating the isotope composition of ET and leaf water enrichment. Further, this effect has also been shown to have a significant influence on the calculations of ^{18}O-CO_2 photosynthetic discrimination and ^{18}O-CO_2 isotope disequilibrium (Griffis et al., 2011).

Finally, Farquhar and Cernusak (2005) proposed a more detailed model of leaf water enrichment at the leaf scale, which accounted for non-steady state behavior and strong leaf water heterogeneity (i.e. the gradient in ^{18}O-H_2O concentration that develops as water moves away from the xylem). In their formulation the Péclet effect accounts for leaf water ^{18}O-H_2O heterogeneity by allowing diffusion of ^{18}O-H_2O molecules against the direction of the mass flux,

$$\delta_{L,b} = \delta_{L,b}^s - \frac{\alpha_k \alpha_{eq} r_t}{w_i} \frac{1 - e^{-P}}{P} \frac{d(W(\delta_{L,b} - \delta_x))}{dt} \tag{16}$$

where P represents the Péclet effect and d/dt is the time rate derivative.

While Barbour et al. (2000) provide compelling evidence for the Péclet effect at the leaf scale, recent works by Xiao et al. (2010, 2012) have shown that optimization of the Péclet parameters (effective length scale) results in anomalously small values, effectively zero, when applied at the canopy scale. They concluded that the leaf-scale physics do not have an analog at the canopy scale (i.e. this same diffusional pathway cannot take place within the canopy airspace, but rather is restricted to individual leaves).

5.4. Partitioning evapotranspiration

A considerable amount of research has been devoted to estimating the sources of water (recent precipitation, ground water, stream water, fog, dew) used by plants and ecosystems and partitioning evapotranspiration into its components (soil evaporation, transpiration) (Dawson and Ehleringer, 1991; Flanagan et al., 1991; Yakir and Wang, 1996; Dawson et al., 2002). The ability to trace the flow of water through the hydrological cycle using stable isotopes provides an opportunity to better understand how ecosystem water use will respond to environmental changes and

the potential implications for ecosystem function. Here, recent progress in partitioning canopy scale ET is reviewed.

Yepez et al. (2003) partitioned ET into its overstory (Mesquite)/understory (C_4 grasses) components in a semi-arid savanna woodland in southeastern Arizona. In their approach, they collected water vapor in flasks from sample inlets at multiple heights within the understory and the overstory. Over the course of three measurement campaigns, lasting about 2-h each, they collected and analyzed approximately 50 flask samples for δ^2H-H_2O and δ^{18}O-H_2O using IRMS. Although the sample number is very limited when considering the dynamic nature of atmospheric water vapor and ET, the amount of effort required to collect such data on a routine basis is substantial. The isotope composition of ET above the understory and within the overstory was then estimated using the traditional Keeling mixing line approach by assuming, somewhat optimistically, little turbulent mixing of vapor between the understory and overstory. Isotopic steady state near midday was assumed so that the isotope composition of transpiration could be derived from direct measurements of δ_x. From simple isotopic mass balance considerations they determined that transpiration accounted for about 85% of ET during the post monsoon season, implying that mesquite trees effectively avoid moisture stress by accessing deep water sources.

Williams et al. (2004) combined eddy covariance water vapor flux measurements with profiles of the isotope composition (δ^2H-H_2O) of water vapor in an olive plantation to partition ET into its components and compared the results against an independent method involving sap flux measurements. In their approach, they captured water vapor in flasks and used the Keeling plot method to estimate the isotope composition of ET. The isotope composition of transpiration was based on the isotope composition of twig water by assuming steady state conditions. Further, they used the Craig–Gordon model (Craig and Gordon, 1965) to approximate the isotope composition of soil evaporation. Here, important assumptions must be made regarding the appropriate kinetic fractionation factors for varying soil moisture characteristics with higher kinetic fractionation effects observed under drier soil conditions. Their study showed that transpiration accounted for nearly 100% of ET during dry periods and that soil evaporation accounted for 69–86% of the midday flux following precipitation events. Although their study period was relatively short (15 days) due to logistical constraints, the results suggested that optical isotope measurements at this site could be used for routine measurement of the isotope fluxes and partitioning of evapotranspiration.

Lee et al. (2007) have provided the first comprehensive and relatively long-term measurement of the isotope composition of ET using the TDLAS and flux ratio approach. Their study was conducted over a mixed deciduous forest in Connecticut over an entire growing season and revealed the major controls on the isotope composition of ET and also tracked the changes in the source water contributing to ET. The isotope composition of ET was very dynamic and the use of a simple model sensitivity analysis revealed that large fluctuations in δ_{ET} could be linked to short-term variations in canopy surface relative humidity and longer timescale changes in the leaf water turnover rate (related directly to the magnitude of ET). In essence, the largest variations in the isotope composition of ET were associated with long turnover time of leaf water amplified by high values of relative humidity. This covariation of relative humidity and evaporative flux resulted in non-steady state behavior so that using isotope composition of ET for flux partitioning was challenging, at least on shorter timescales. Their seasonal analyses of the isotope water budget for the forest revealed important seasonal changes in water use. The early growing season isotope fluxes showed that ET was closely coupled to recent rainfall, while late growing season ET was more strongly linked to "older" (deeper) water sources. Their study provides further confirmation that forest systems rely on multiple water sources to avoid drought. Quantifying these changes in forest water use represents an important step toward developing and improving land surface models that simulate the coupled carbon and water flows.

Wang et al. (2010) have also examined the ET partitioning problem, but under relatively controlled environmental conditions. In their work, they made use of TDLAS water vapor measurements within the biosphere 2 research facility in Arizona to examine ET partitioning along a gradient of woody plant cover. They used the relatively high frequency water vapor isotope measurements and the Keeling plot approach to estimate the isotope composition of ET and used a leaf chamber to estimate the isotope composition of transpiration. Their work showed considerable promise and relatively good agreement (to within 15%) with the partitioning derived from lysimeter and sap flow measurements. As expected, their measurements showed that soil evaporation increased with decreasing plant density.

These recent applications demonstrate the feasibility of combining isotope and micrometeorological techniques to partition ET and that fast optical isotope observations have improved our capacity to carry out these types of investigations by providing near-continuous estimates of the isotope composition of ET. However, some key issues remain. An important challenge is capturing the dynamic variation in the isotope composition of soil evaporation and transpiration (end members). It would appear from the above studies that the isotope partitioning strategy is better suited to more arid environments with sparse vegetation. Our own work in agricultural ecosystems indicates that the soil evaporation component is small (<10%) so that the precision in the isotope partitioning method cannot resolve such small differences. Similarly, in a Eucalyptus forest the additional information provided by measuring profiles of δ^2H-H_2O did not reduce the uncertainty in the partitioning of ET (Haverd et al., 2011). Further, a major limitation is determining the dynamic variation in the soil water isotope content and the appropriate kinetic fractionation effects at the soil–atmosphere interface (Braud et al., 2009a,b).

5.5. Coupled water and carbon cycle

The isotope composition of the leaf water plays a key role in determining the oxygen isotope composition of CO_2 in leaves. Table 4 provides examples of the variability that can be expected under field conditions. As CO_2 diffuses into stomata and goes into solution at the chloroplast it isotopically equilibrates according to the hydration reaction (Hesterburg and Siegenthaler, 1991):

$$H_2^{18}O(l) + CO_2(g) \rightarrow H^+ + [HCO_2^{18}O]^-(aq) \rightarrow H_2O(l) + CO^{18}O(g) \quad (17)$$

The extent of equilibration and, therefore, the ^{18}O-CO_2 enrichment in leaves varies among C_3 and C_4 species due to the relative extent of CO_2–H_2O equilibration related to carbonic anhydrase (CA) activity (Gillon and Yakir, 2001). Early experimental observations indicated that isotope equilibration was nearly complete in C_3 species, but significantly lower in C_4 species. These differences between photosynthetic pathway have been identified as a potential signal that can be used to evaluate how land use change is impacting the oxygen isotope content of CO_2 and O_2 in the atmosphere. These differences are also required in order to estimate global gross ecosystem photosynthesis (GEP). Observations at the canopy scale, however, remain extremely sparse.

The photosynthetic ^{18}O-CO_2 fractionation ($^{18}\Delta$) using a big-leaf analogy can be described as (Yakir, 2003):

$$^{18}\Delta \approx \epsilon_k^c + \frac{C_c}{C_a - C_c}\left[\theta_{eq}(\delta_{L,e}^c - \delta_a) - (1-\theta_{eq})\epsilon_k^c / \left(\frac{C_c}{C_a - C_c} + 1\right)\right] \quad (18)$$

where $\delta_{L,e}^c = \epsilon_{eq}^c + \delta_{L,e}$ (reported on the VPDB scale), ϵ_k^c is the kinetic fractionation factor for ^{18}O-CO_2, C_a and C_c represent the CO_2 concentration in the surface layer and the leaf chloroplast, the fraction $(C_c/(C_a - C_c))$ describes the retroflux of ^{18}O-CO_2, and θ_{eq} is the canopy scale CO_2 hydration efficiency (ranging from 0 to 1 depending on species and photosynthetic pathway).

Xiao et al. (2010) recently combined field-scale flux measurements of ^{18}O-CO_2 and ^{18}O-H_2O and the Simple Isotope Land Surface Scheme (SiLSM) to examine the biophysical controls on the ^{18}O-CO_2 exchange. In their study they used soybean as a model C_3 ecosystem. Model optimization revealed that the extent of ^{18}O equilibration at the canopy scale was significantly lower than that observed in leaf-scale studies. Their CO_2 hydration value was approximately 0.46, less than half the value reported at the leaf-scale. In a separate study conducted for a C_4 corn canopy, Griffis et al. (2011) showed that the CO_2 hydration efficiency at the canopy scale was significantly lower than that of C_4 leaf-scale studies (i.e. 0.19 versus 0.70). These field-scale results imply that only 20–50% of the ^{18}O-CO_2 retroflux is isotopically equilibrated (i.e. relabeled) with the leaf water isotope signal. Overestimating the CO_2 hydration efficiency will lead to a significant underestimate of GEP based on inverse-type analyses (Yakir, 2003).

The mechanism underlying the lower canopy-scale CO_2 hydration efficiency is not yet clear. Cousins et al. (2006) have shown in lab studies that the CO_2 hydration efficiency decreases significantly under high light conditions. Griffis et al. (2011) have shown that CO_2 hydration efficiency of C_4 corn leaves growing under field conditions tended to be lower at the top of the canopy, but overall, were substantially larger than the canopy-scale estimates. Leaf-level experiments on a variety of C_4 grasses by Cousins et al. (2008) indicated that CA activity could not be used to reliably predict the extent of ^{18}O equilibration between leaf H_2O and CO_2. They proposed two explanations including: (1) CA is not isolated to the sites of CO_2–H_2O exchange so that there may be a weak relation among these variables; and (2) the estimate of the isotope ratio of H_2O at the site of evaporation may be in error because this quantity cannot be measured directly.

Recent findings also show that CA may play a significant role in influencing the isotope composition of net soil respiration (Seibt et al., 2006; Wingate et al., 2009). Increasing evidence indicates that many soil microorganisms (bacterial, fungal, etc.) produce the CA enzyme. Wingate et al. (2009) have shown that CO_2 hydration in soils is typically faster than the uncatalyzed rate, which has been traditionally assumed. Based on soil profile information and chamber isoflux data, they have shown that CA enhances the rate of hydration by 10–300 times. The highest rates were observed at Mediterannean and tropical sites. The implications are that CO_2 diffusing from soil and into the atmosphere will have a more enriched isotopic signal than previously thought because of the stronger equilibration near the soil surface, where strong evaporative enrichment occurs. By including this new biophysical mechanism into a global isotope-enabled model, Wingate et al. (2009) have shown that observed latitudinal gradient in ^{18}O-CO_2 can be better explained/reproduced.

It is interesting to note that either enhanced CA activity in the soil or weaker CA activity in canopy photosynthesis would influence atmospheric ^{18}O-CO_2 signatures in the same direction. Overall, further research is required in order to understand how CA activity influences both photosynthetic and respiratory discrimination under field conditions and at the canopy scale. This may prove particularly relevant when attempting to explain the large global GEP estimate proposed by Welp et al. (2011) or if attempting to partition net ecosystem CO_2 exchange at the field scale using the oxygen isotope tracer approach. It is clear from the recent literature that the ^{18}O-CO_2 disequilibrium between respiration and photosynthesis is much stronger than for ^{13}C-CO_2 (Table 3) and that it decreases with increasing precipitation frequency and magnitude (Wingate et al., 2010a; Griffis et al., 2011; Sturm et al., 2012). This larger disequilibrium should prove favorable for partitioning F_N, however, to date this has not been fully realized because of the measurement challenges. Simultaneous fast optical isotope measurements of the water vapor and carbon dioxide fluxes and isotope end members are required.

6. Future directions

It is remarkable that energy, water, and carbon fluxes are now measured at more than 500 sites globally on a near continuous basis. This development occurred relatively rapidly through the late 1980s and 1990s as cheaper and more robust sonic anemometers and IRGAs were developed for remote field applications. Baldocchi (2008) highlighted a number of important findings regarding the global carbon cycle that could only have been realized from such a network. We are now aware that the timing of snowmelt and subtle changes in phenology can have profound impacts on ecosystem carbon budgets. Results from the network demonstrate that it is the change in length of growing season that has the greatest impact on carbon sequestration – not the variation in photosynthetic capacity. Old-growth forests, once thought to be carbon neutral or weak sources, are in many cases continuing to sequester significant amounts of carbon on an annual basis. Further, respiration and photosynthesis have been found to respond in unexpected ways to high temperatures, drought, and precipitation events.

Isotope observations remain relatively rare within the Fluxnet network and have been limited to intensive campaigns of short duration. However, with the rapid development of laser-based technologies that are field-deployable, it is likely that these measurements will be incorporated at many sites in the near future. The National Ecological Observatory Network (NEON, http://www.neoninc.org/) is planning to make continuous isotope measurements of CO_2 and water vapor at each of its network sites using these new technologies. Such measurements should expand our capabilities to study and interpret the biophysical processes influencing the carbon and water budgets at the ecosystem, regional, and continental scales. There will also be opportunities to link these surface and boundary layer observations with advances in satellite-based isotope observations – at least in terms of water vapor (Worden et al., 2006, 2007; Herbin et al., 2007; Brown et al., 2008).

The literature reviewed above indicates that there is significant potential to improve our understanding of the biophysical processes governing the exchange of carbon and water between the land and atmosphere. Here I highlight four areas that offer the promise of new scientific insights.

First, there is a need for continuous carbon isotope measurements of ecosystem and chamber-scale respiration to better understand these complex processes. This seems especially promising in light of compound-specific carbon isotope measurements of sugars, etc. in phloem sap, which can be used to help interpret these signals. It is likely that network-wide analysis of compound specific carbon isotope ratios in relation to ecosystem scale observations of ecosystem respiration will reveal important new insights regarding the influence of phenology, temperature extremes, drought, and precipitation events on both autotrophic

and heterotrophic respiration. These types of data and analyses could be used to develop more sophisticated algorithms of respiration in land-atmosphere surface schemes.

Second, with the new capacity to measure ecosystem-scale ^{18}O-H_2O and ^{18}O-CO_2 fluxes, there is new potential to provide an independent constraint on ecosystem scale photosynthesis and respiration and to better understand the processes influencing the ^{18}O composition of the atmosphere. Recent work by Welp et al. (2011) suggests that global ecosystem production (GEP) is significantly larger (170 Gt) than previously (120 Gt) thought. Their conclusion was reached based on the analysis of the high-precision ^{18}O-CO_2 global flask network data. The literature reviewed above indicates that interpretation of ^{18}O-CO_2 fluxes and discrimination requires a robust estimate of the leaf water enrichment at the canopy scale and good understanding of how CA influences the ^{18}O equilibration in both leaves and soils. To date, the only studies that have simultaneously made these types of measurements at the ecosystem scale have been in agricultural systems. Similar measurements are planned at all NEON sites and have significant potential to help us resolve the extent of CO_2 hydration efficiency across a broad array of systems and to provide independent estimates of ecosystem scale photosynthesis and respiration. These studies could be compared with the analysis of Welp et al. (2011) to help better understand the disparity in the estimates of global GEP. Further, with recent advances in optical isotope techniques and new process understanding of ^{18}O-H_2O and ^{18}O-CO_2 exchange there is new opportunity to re-evaluate the feasibility of partitioning F_N.

Third, given the small ^{13}C-CO_2 disequilibrium between respiration and photosynthesis and the inherent noise in determining the ecosystem-scale carbon isotope fluxes, a powerful way forward is to increase the use of ^{13}C-CO_2 labeling studies under field conditions (Epron et al., 2012). Plain et al. (2009) were one of the first to combine a TDLAS isotope system and isotope labeling approach to trace the flow of carbon on a near-continuous basis within a beech forest in France. In their experiment, they developed a large flexible canopy chamber to fumigate two individual beech trees with nearly pure ^{13}C-CO_2 for a 3-h pulse in late September. The isotope ratio of the chamber-canopy air was highly enriched in ^{13}C-CO_2 (initially >400,000‰). Small tree bole and soil chambers were connected to the TDLAS for near-continuous measurement of the CO_2 efflux and its carbon isotope ratio in order to determine lags in carbon transport and its half-life. Immediately following the isotope fumigation (<1 h) they were able to detect significant enrichment of ^{13}C-CO_2 in the bole and soil respiration. The peak in enrichment (>900‰) for the soil CO_2 efflux was observed within 72–84 h and lagged bole respiration by about 9 h. Continuous measurement over a two month period (the chase period) showed a very distinct pattern that was best fit using a double-exponential relation that was used to help describe the "fast" and "slow" processes at work. The second peak in their chase period data (the so-called slow processes) provides evidence for transitory storage or remobilization of carbon and deserves further examination. Investigating these processes in long-term experiments that account for phenological variation and seasonal variation in climate should yield important new insights on ecosystem respiration. Further, given isotope enabled models such as SiLSM and the Community Land Model (CLM-CN 3.5), isotope labeling studies can be used to test the respiration, carbon allocation, and carbon pool strategies of such models. For example, Fig. 8 shows an example of a virtual isotope tracer experiment using CLM and illustrates how the photosynthetic signal (here we spiked the model atmosphere with a highly enriched ^{13}C-CO_2 concentration) is eventually incorporated into the SOM pools and how the signal dissipates with time since the isotope enrichment. These type of field isotope tracer experiments can provide a powerful way to assess and tune the algorithms that describe respiration in isotope-enabled ecosystem models.

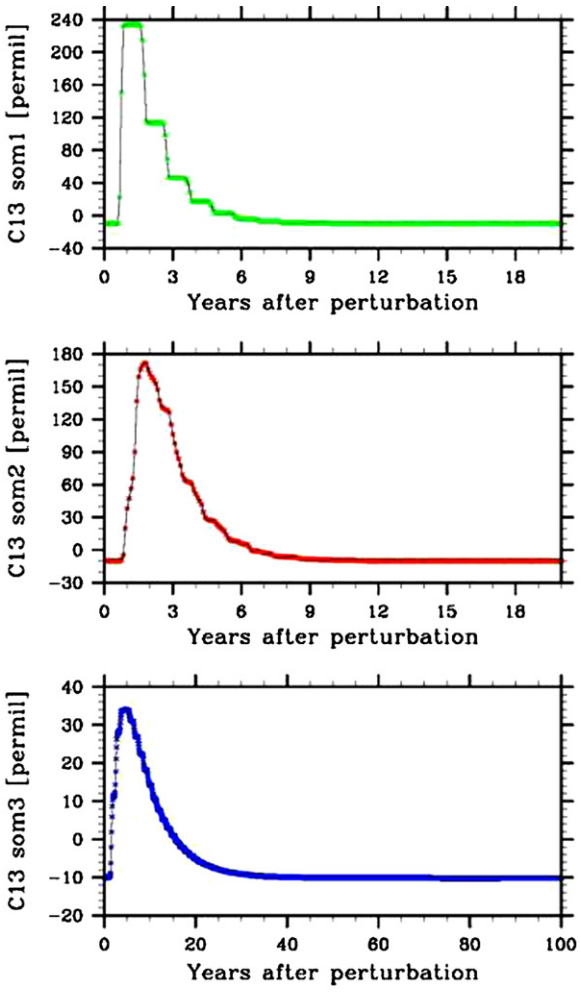

Fig. 8. Virtual isotope tracer experiments using the Community Land Model (CLM v3.5). This virtual experiment was conducted for a C_4 corn crop growing in Minnesota. The *y*-axes show the isotope enrichment in three soil organic matter pools represented in the model. For example, the top panel (SOM pool 1) exhibits the fastest carbon turnover time. SOM pool 2 and SOM pool 3 represent the intermediate and slow carbon turnover times within the CLM model framework. The *x*-axes indicate the elapsed time following the model atmospheric perturbation of $^{13}CO_2$. The result is sensitive to the dose and duration of the $^{13}CO_2$ perturbation.

Finally, optical isotope techniques for the measurement of carbon and hydrogen isotopes in methane and nitrogen and oxygen isotopes in nitrous oxide (including isotopologues and isotopomers) are becoming available. These new techniques may offer new capacity to study the environmental controls on methane production/consumption and denitrification/nitrification at unprecedented temporal and spatial scales. The recent work of Santoni et al. (2012) has demonstrated the feasibility of using TDLAS to measure the isoflux of methane, which should lead to new insights regarding the environmental controls on methane budgets, methanogenesis, and ebullition events in wetlands and peatlands.

Acknowledgments

I would like to thank my close collaborators (John Baker, Xuhui Lee, and Steve Sargent), students (Jianmin Zhang, Joel Fassbinder, Natalie Schultz, Kaycie Billmark, and Ming Chen) and technicians (Matt Erickson and Jeremy Smith) for all of their help and contributions to our isotope research over the past 10 years. I also thank David Bowling, David Griffith, Margaret Barbour, Stephen

Parkes, and Felix Vogel for their valuable insights and discussion related to this work. This research has been supported by the National Science Foundation, ATM-0546476 (T.G.) and a Faculty Development Grant from the College of Food, Agricultural, and Natural Resource Sciences, University of Minnesota.

References

Amundson, R., Stern, L., Baisden, T., Wang, Y., 1998. The isotope composition of soil and soil-respired CO_2. Geoderma 82, 83–114.

Aranibar, J.N., Berry, J.A., Riley, W.J., Pataki, D.E., Law, B.E., Ehleringer, J.R., 2006. Combining meteorology, eddy fluxes, isotope measurements, and modeling to understand environmental controls of carbon isotope discrimination at the canopy scale. Glob. Change Biol. 12, 710–730.

Badeck, F.-W., Tcherkez, G., Nogués, S., Piel, C., Ghashghaie, J., 2005. Post-photosynthetic fractionation of stable carbon isotopes between plant organs – a widespread phenomenon. Rapid Commun. Mass Spectrom. 19, 1381–1391.

Bai, M., Kostler, M., Kunstmann, J., Wilske, B., Gattinger, A., Frede, H.-G., Breuer, L., 2011. Biodegradability screening of soil amendments through coupling of wavelength-scanned cavity ring-down spectroscopy to multiple dynamic chambers. Rapid Commun. Mass Spectrom. 25, 3683–3689.

Baldocchi, D., 2008. Breathing of the terrestrial biosphere: lessons learned from a global network of carbon dioxide flux measurement systems. Aust. J. Plant Bot. 56, 1–26.

Barbour, M., Schurr, U., Henry, B., Wong, S., Farquhar, G., 2000. Variation in the oxygen isotope ratio of phloem sap sucrose from castor bean. Evidence in support of the Peclet effect. Plant Physiol. 123, 671–679.

Barbour, M.M., Farquhar, G.D., Hanson, D.T., Bickford, C.P., Powers, H., McDowell, N.G., 2007. A new measurement technique reveals temporal variation in delta O-18 of leaf-respired CO_2. Plant Cell Environ. 30, 456–468.

Barbour, M.M., Hunt, J.E., Kodama, N., Laubach, J., McSeveny, T.M., Rogers, G.N., Tcherkez, G., Wingate, L., 2011. Rapid changes in $\delta^{13}C$ of ecosystem-respired CO_2 after sunset are consistent with transient ^{13}C enrichment of leaf respired Co_2. New Phytol. 190, 990–1002.

Bariac, T., Rambal, S., Jusserand, C., Berger, A., 1989. Evaluating water fluxes of field-grown alfalfa from diurnal observations of natural isotope concentrations, energy budget and ecophysiological parameters. Agric. Forest Meteorol. 48, 263–283.

Bathellier, C., Badeck, F.-W., Couzi, P., Harscoët, S., Mauve, C., Ghashghaie, J., 2008. Divergence in $\delta^{13}C$ of dark respired CO_2 and bulk organic matter occurs during the transition between heterotrophy and autotrophy in *Phaseolus vulgaris* plants. New Phytol. 177, 406–418.

Becker, J., Sauke, T., Loewenstein, M., 1992. Stable isotope analysis using tunable diode laser spectroscopy. Appl. Opt. 31, 1921–1927.

Bender, M., Sowers, T., Labeyrie, L., 1994. The dole effect and its variations during the last 130,000 years as measured in the vostok ice core. Glob. Biogeochem. Cycl. 8, 363–376.

Bickford, C.P., Mcdowell, N.G., Erhardt, E.B., Hanson, D.T., 2009. High-frequency field measurements of diurnal carbon isotope discrimination and internal conductance in a semi-arid species, *Juniperus monosperma*. Plant Cell Environ. 32 (July (7)), 796–810.

Billmark, K., Griffis, T., 2009. Influence of phenology and land management on biosphere–atmosphere isotopic CO_2 exchange. In: Phenology of Ecosystem Processes: Applications in Global Change Research. Springer Science and Business Media, pp. 143–166.

Blanken, P.D., Black, T.A., Neumann, H.H., den Hartog, G., Yang, P.C., Nesic, Z., Staebler, R., Chen, W., Novak, M.D., 1998. Turbulent flux measurements above and below the overstory of a boreal aspen forest. Bound. Layer Meteorol. 89 (1), 109–140.

Bowling, D.R., Baldocchi, D.D., Monson, R.K., 1999. Dynamics of isotopic exchange of carbon dioxide in a Tennessee deciduous forest. Glob. Biogeochem. Cycl. 13 (4), 903–922.

Bowling, D.R., Burns, S.P., Conway, T.J., Monson, R.K., White, J.W.C., 2005. Extensive observations of CO_2 carbon isotope content in and above a high-elevation subalpine forest. Glob. Biogeochem. Cycl. 19 (3), 15–83.

Bowling, D.R., Massman, W.J., 2011. Persistent wind-induced enhancement of diffusive CO_2 transport in a mountain forest snowpack. J. Geophys. Res. Biogeosci., 116.

Bowling, D.R., McDowell, N.G., Welker, J.M., Bond, B.J., Law, B.E., Ehleringer, J.R., 2003a. Oxygen isotope content of CO_2 in nocturnal ecosystem respiration: 2. Short-term dynamics of foliar and soil component fluxes in an old-growth ponderosa pine forest. Glob. Biogeochem. Cycl. 17, 1124.

Bowling, D.R., Pataki, D.E., Randerson, J.T., 2008. Carbon isotopes in terrestrial ecosystem pools and CO_2 fluxes. New Phytol. 178, 24–40.

Bowling, D.R., Sargent, S., Tanner, B., Ehleringer, J.R., 2003b. Tunable diode laser absorption spectroscopy for stable isotope studies of ecosystem-atmosphere CO_2 exchange. Agric. Forest Meteorol. 118 (4), 1–19, 81.

Bowling, D.R., Tans, P.P., Monson, R.K., 2001. Partitioning net ecosystem carbon exchange with isotopic fluxes of CO_2. Glob. Change Biol. 7 (2), 127–145.

Brand, W., Geilmann, H., Crosson, E., Rella, C., 2009. Cavity ring-down spectroscopy versus high-temperature conversion isotope ratio mass spectrometry; a case study on delta H-2 and delta O-18 of pure water samples and alcohol/water mixtures. Rapid Commun. Mass Spectr. 23, 1879–1884.

Braud, I., Bariac, T., Biron, P., Vauclin, M., 2009a. Isotopic composition of bare soil evaporated water vapor. Part II: modeling of RUBIC IV experimental results. J. Hydrol. 369 (May (1–2)), 17–29.

Braud, I., Biron, P., Bariac, T., Richard, P., Canale, L., Gaudet, J.P., Vauclin, M., 2009b. Isotopic composition of bare soil evaporated water vapor. Part I: RUBIC IV experimental setup and results. J. Hydrol. 369 (May (1–2)), 1–16.

Brown, D., Worden, J., Noone, D., 2008. Comparison of atmospheric hydrology over convective continental regions using water vapor isotope measurements from space. J. Geophys. Res. Atmos. 113 (D15), http://dx.doi.org/10.1029/2007JD009676123.

Buchmann, N., Brooks, J., Flanagan, L., Ehleringer, J., 1998. Carbon isotope discrimination of terrestrial ecosystems. In: Stable Isotopes. Oxford, pp. 203–221.

Cappa, C., Hendricks, M., DePaolo, D., Cohen, R., 2003. Isotopic fractionation of water during evaporation. J. Geophys. Res. Atmos. 108, 4525.

Ciais, P., Tans, P.P., White, J.W.C., Trolier, M., Francey, R.J., Berry, J.A., Randall, D.R., Sellers, P.J., Collatz, J.G., Schimel, D.S., 1995. Partitioning of ocean and land uptake of CO_2 as inferred by $\delta^{13}C$ measurements from the NOAA Climate Monitoring and Diagnostics Laboratory Global Air Sampling network. J. Geophys. Res. 100, 5051–5070.

Cohn, M., Urey, H., 1938. Oxygen exchange reactions of organic compounds and water. J. Am. Chem. Soc. 60, 679–687.

Coleman, M., Shepherd, T., Durham, J., Rouse, J., Moore, G., 1982. Reduction of water with zinc for hydrogen isotope analysis. Anal. Chem. 54, 993–995.

Coplen, T., 1994. Reporting of the stable hydrogen, carbon, and oxygen isotopic abundances. Pure Appl. Chem. 66, 273–276.

Coplen, T., 2011. Guidelines and recommended terms for expression of stable-isotope-ratio and gas-ratio measurement results. Rapid Commun. Mass Spectrom. 25, 2538–2560.

Corrsin, S., 1974. Limitations of gradient transport models in random walks and turbulence. In: Turbulent Diffusion in Environmental Pollution. Academic Press, pp. 25–60.

Cousins, A., Badger, M., von Caemmerer, S., 2006. A transgenic approach to understanding the influence of carbonic anhydrase on c18oo discrimination during C4 photosynthesis. Plant Physiol. 142, 662–672.

Cousins, A., Badger, M., von Caemmerer, S., 2008. C4 photosynthetic isotope exchange in NAD-ME- and NADP-ME-type grasses. J. Exp. Bot. 59, 1695–1703.

Craig, H., Gordon, L., 1965. Deuterium and oxygen-18 variations in the ocean and the marine atmosphere. In: Tongiorgi, E. (Ed.), Proceedings of a Conference on Stable Isotopes in Oceanographic Studies and Paleotemperatures. July, Spoleto, Italy, pp. 9–130.

Crosson, E.R., Ricci, K.N., Richman, B.A., Chilese, F.C., Owano, T.G., Provencal, R.A., Todd, M.W., Glasser, J., Kachanov, A.A., Paldus, B.A, Spence, T.G., Zare, R.N., 2002. Stable isotope ratios using cavity ring-down spectroscopy: determination of 13C/12C for carbon dioxide in human breath. Anal. Chem. 74, 2003–2007.

Davidson, E., Savage, K., Verchot, L., Navarro, R., 2002. Minimizing artefacts and biases in chamber-based measurements of soil respiration. Agric. Forest Meteorol. 113, 21–37.

Dawson, T., Brooks, P., 2001. Fundamentals of stable isotope chemistry and measurement. In: Stable Isotope Techniques in the Study of Biological Processes and Functioning of Ecosystems. Kluwer Academic Publishers, pp. 1–18.

Dawson, T., Ehleringer, J., 1991. Streamside trees that do not use stream water. Nature 350, 335–337.

Dawson, T., Mambelli, S., Plamboeck, A., Templer, P., Tu, K., 2002. Stable isotopes in plant ecology. Annu. Rev. Ecol. Syst. 33, 507–559.

DeBievre, P., Gallet, M., Holden, N.E., Barnes, I.L., 1984. Isotopic abundances and atomic weights of the elements. J. Phys. Chem. Ref. Data 13, 809–891.

Denmead, O., Bradley, E., 1985. Flux–gradient relationships in a forest canopy. In: The Forest–Atmosphere Interaction. Reidel Publishing Co, pp. 421–442.

Dole, M., Lane, G., Rudd, D., Zaukelies, D., 1954. Isotopic composition of atmospheric oxygen and nitrogen. Geochim. Cosmochim. Acta 6, 65–78.

Dongmann, G., Nurnberg, H., Forstel, H., Wagener, K., 1974. Enrichment of H218O in leaves of transpiring plants. Radiat. Environ. Biophys. 11, 41–52.

Drewitt, G.B., Wagner-Riddle, C., Warland, J.S., 2009. Isotopic CO_2 measurements of soil respiration over conventional and no-till plots in fall and spring. Agric. Forest Meteorol. 149, 614–622.

Dugan, J., Borthwick, J., Harmon, R., Gagnier, M., Glahn, J., Kinsel, E., Macleod, S., Viglino, J., Hess, J., 1985. Guanidine-hydrochloride method for determination of water oxygen isotope ratios and the O-18 fractionation between carbon-dioxide and water at 25 °C. Anal. Chem. 57 (8), 1734–1736.

Duranceau, M., Ghashghaie, J., Badeck, F., Deleens, E., Cornic, G., 1999. $\delta^{13}C$ of CO_2 respired in the dark in relation to $\delta^{13}C$ of leaf carbohydrates in *Phaseolus vulgaris* L. under progressive drought. Plant Cell Environ. 22 (5), 515–523.

Duranceau, M., Ghashghaie, J., Brugnoli, E., 2001. Carbon isotope discrimination during photosynthesis and dark respiration in intact leaves of *Nicotiana sylvestris*: comparison between wild type and mitochondrial mutant plants. Aust. J. Plant Physiol. 28, 65–71.

Edwards, G.C., Thurtell, G.W., Kidd, G.E., Dias, G.M., Wagner-Riddle, C., 2003. A diode laser based gas monitor suitable for measurement of trace gas exchange using micrometeorological techniques. Agric. Forest Meteorol. 115 (February (1–2)), 71–89.

Epron, D., Bahn, M., Derrien, D., Lattanzi, F.A., Pumpanen, J., Gessler, A., Hoegberg, P., Maillard, P., Dannoura, M., Gerant, D., Buchmann, N., 2012. Pulse-labelling trees to study carbon allocation dynamics: a review of methods, current knowledge and future prospects. Tree Physiol. 32, 776–798.

Epstein, S., Mayeda, T., 1953. Variations of the O18 content of waters from natural sources. Geochim. Cosmochim. Acta 4, 213–224.

Esler, M., Griffith, D., Wilson, S., Steele, L., 2000. Precision trace gas analysis by FT-IR spectroscopy 2. The 13C/12C isotope ratio of CO_2. Anal. Chem. 72, 216–221.
Farquhar, G., Cernusak, L., 2005. On the isotopic composition of leaf water in the non-steady state. Funct. Plant Biol. 32 (4), 293–303.
Farquhar, G.D., 1983. On the nature of carbon isotope discrimination in C_4 species. Aust. J. Plant Physiol. 10 (2), 205–226.
Farquhar, G.D., Ehleringer, J.R., Hubick, K.T., 1989. Carbon isotope discrimination and photosynthesis. Annu. Rev. Plant Physiol. Plant Mol. Biol. 40, 503–537.
Farquhar, G.D., Lloyd, J., Taylor, J.A., Flanagan, L.B., Syvertsen, J.P., Hubick, K.T., Wong, S.C., Ehleringer, J.R., 1993. Vegetation effects on the isotope composition of oxygen in atmospheric CO_2. Nature 363, 439–443.
Farquhar, G.D., von Caemmerer, S., Berry, J.A., 2001. Models of photosynthesis. Plant Physiol. 125 (1), 42–45.
Fassbinder, J., Griffis, T., Baker, J., 2012a. Evaluation of carbon isotope flux partitioning theory under simplified and controlled environmental conditions. Agric. Forest Meteorol. 153, 154–164.
Fassbinder, J., Griffis, T., Baker, J., 2012b. Interannual, seasonal, and diel variability in the carbon isotope composition of respiration in a C_3/C_4 agricultural ecosystem. Agric. Forest Meteorol. 153, 144–153.
Flanagan, L., Cai, T., Black, T.A., Barr, A.G., McCaughey, J.H., Margolis, H., 2012. Measuring and modeling ecosystem photosynthesis and the carbon isotope composition of ecosystem-respired CO_2 in three boreal coniferous forests. Agric. Forest Meteorol. 153, 165–176.
Flanagan, L., Comstock, J., Ehleringer, J., 1991. Comparison of modeled and observed environmental-influences on the stable oxygen and hydrogen isotope composition of leaf water in phaseolus-vulgaris l. Plant Physiol. 96, 588–596.
Flanagan, L.B., Ehleringer, J.R., 1998. Ecosystem-atmosphere CO_2 exchange: interpreting signals of change using stable isotope ratios. Trends Ecol. Evol. 13 (1), 10–14.
Francey, R.J., Allison, C.E., Etheridge, D.M., Trudinger, C.M., Enting, I.G., Leuenberger, M., Langenfelds, R.L., Michel, E., Steele, L.P., 1999. A 1000-year high precision record of $\delta^{13}C$ in atmospheric CO_2. Tellus B 51 (2), 170–193.
Francey, R.J., Tans, P.P., 1987. Latitudinal variation in oxygen-18 of atmospheric CO_2. Nature 327, 495–497.
Fratini, G., Ibrom, A., Arriga, N., Burba, G., Papale, D., 2012. Relative humidity effects on water vapour fluxes measured with closed-path eddy-covariance systems with short sampling lines. Agric. Forest Meteorol. 165, 53–63.
Fung, I., Field, C.B., Berry, J.A., Thompson, M.V., Randerson, J.T., Malmstrom, C.M., Vitousek, P.M., Collatz, G.J., Sellers, P.J., Randall, D.A., Denning, A.S., Badeck, F., John, J., 1997. Carbon 13 exchanges between the atmosphere and biosphere. Glob. Biogeochem. Cycl. 11 (4), 507–533.
Gessler, A., Keitel, C., Kodama, N., Weston, C., Winters, A.J., Keith, H., Grice, K., Leuning, R., Farquhar, G.D., 2007. $\delta^{13}C$ of organic matter transported from leaves to the roots in *Eucalyptus delegatensis*: short-term variations and relation to respired CO_2. Funct. Plant Biol. 34, 692–706.
Gessler, A., Tcherkez, G., Karyanto, O., Keitel, C., Ferrio, J.P., Ghashghaie, J., Kreuzwieser, J., Farquhar, G.D., 2009. On the metabolic origin of the carbon isotope composition of CO_2 evolved from darkened light-acclimated leaves in Ricinus communis. New Phytol. 181 (2), 374–386.
Ghashghaie, J., Badeck, F.-W., Lanigan, G., Nogués, S., Tcherkez, G., Deleens, E., Cornic, G., Griffiths, H., 2003. Carbon isotope fractionation during dark respiration and photorespiration in C_3 plants. Phytochem. Rev. 2, 145–161.
Ghashghaie, J., Duranceau, M., Badeck, F.W., Cornic, G., Addeline, M.T., Deleens, E., 2001. $\delta^{13}C$ of CO_2 respired in the dark in relation to $\delta^{13}C$ of leaf metabolites: comparison between *Nicotiana sylvestris* and *Helianthus annuus* under drought. Plant Cell Environ. 24, 505–515.
Gianfrani, L., Gagliardi, G., van Burgel, M., Kerstel, E., 2003. Isotope analysis of water by means of near-infrared dual-wavelength diode laser spectroscopy. Opt. Expr. 11, 1566–1576.
Giauque, W., Johnson, H., 1929a. An isotope of oxygen, mass 18. J. Am. Chem. Soc. 51, 1436–1441.
Giauque, W., Johnson, H., 1929b. An isotope of oxygen of mass 17 in the earth's atmosphere. Nature 123, 831.
Gillon, J., Yakir, D., 2001. Influence of carbonic anhydrase activity in terrestrial vegetation on the O-18 content of atmospheric CO_2. Science 291, 2584–2587.
Glenn, A.J., Amiro, B.D., Tenuta, M., Wagner-Riddle, C., Drewitt, G., Warland, J., 2011. Contribution of crop residue carbon to soil respiration at a northern prairie site using stable isotope flux measurements. Agric. Forest Meteorol. 151 (August (8)), 1045–1054.
Good, S.P., Soderberg, K., Wang, L., Caylor, K.K., 2012. Uncertainties in the assessment of the isotopic composition of surface fluxes: a direct comparison of techniques using laser-based water vapor isotope analyzers. J. Geophys. Res. Atmos. 117, http://dx.doi.org/10.1029/2011JD017168.
Grayson, M., 1992. Professor al nier and his influence on mass spectrometry. J. Am. Soc. Mass Spectrom. 3, 685–694.
Griffis, T.J., Sargent, S.D., Lee, X., Baker, J.M., Greene, J., Erickson, M., Zhang, X., Billmark, K., Schultz, N., Xiao, W., Hu, N., 2010. Determining the oxygen isotope composition of evapotranspiration using eddy covariance. Bound. Layer Meteorol. 137 (2), 307–326.
Griffis, T., Lee, X., Baker, J., Sargent, S., Schultz, N., Erickson, M., Zhang, X., Fassbinder, J., Billmark, K., Xiao, W., Hu, N., 2011. Oxygen isotope composition of evapotranspiration and its relation to C_4 photosynthetic discrimination. J. Geophys. Res. Biogeosci. 116, G01035.
Griffis, T.J., Baker, J.M., Sargent, S.D., Tanner, B.D., Zhang, J., 2004. Measuring field-scale isotopic CO_2 fluxes with tunable diode laser absorption spectroscopy and micrometeorological techniques. Agric. Forest Meteorol. 124 (1–2), 15–29, 38.
Griffis, T.J., Lee, X., Baker, J.M., Sargent, S.D., King, J.Y., 2005a. Feasibility of quantifying ecosystem-atmosphere $C^{18}O^{16}O$ exchange using laser spectroscopy and the flux–gradient method. Agric. Forest Meteorol. 135 (1–4), 44–60.
Griffis, T.J., Baker, J.M., Zhang, J., 2005b. Seasonal dynamics and partitioning of isotopic CO_2 Exchange in a C_3/C_4 managed ecosystem. Agric. Forest Meteorol. 132, 1–19.
Griffis, T.J., Sargent, S.D., Baker, J.M., Lee, X., Tanner, B.D., Greene, J., Swiatek, E., Billmark, K., 2008. Direct measurement of biosphere–atmosphere isotopic CO_2 exchange using the eddy covariance technique. J. Geophys. Res. 113, D08304.
Griffis, T.J., Zhang, J., Baker, J.M., Kljun, N., Billmark, K., 2007. Determining carbon isotope signatures from micrometeorological measurements: implications for studying biosphere–atmosphere exchange processes. Bound. Layer Meteorol. 123 (2), 295–316.
Griffith, D., Deutscher, N., Caldow, C., Kettlewell, G., Riggenbach, M., Hammer, S., 2012. A fourier transform infrared trace gas analyzer for atmospheric applications. Atmos. Measur. Tech. 5, 2481–2498.
Griffith, D., Jamie, I., Esler, M., Wilson, S., Parkes, S., Waring, C., Bryant, G., 2006. Real-time field measurements of stable isotopes in water and CO_2 by FTIR spectrometry. Isot. Environ. Health Stud. 42, 9–20.
Guillon, S., Pili, E., Agrinier, P., 2012. Using a laser-based CO_2 carbon isotope analyzer to investigate gas transfer in geological media. Appl. Phys. B 107, 449–457.
Gulbranson, E., Nier, A., 1939. Variations in the relative abundance of the carbon isotopes. J. Am. Chem. Soc. 61, 697–698.
Haverd, V., Cuntz, M., Griffith, D., Keitel, C., Tadros, C., Twining, J., 2011. Measured deuterium in water vapour concentration does not improve the constraint on the partitioning of evapotranspiration in a tall forest canopy, as estimated using a soil vegetation atmosphere transfer model. Agric. Forest Meteorol. 151, 645–654.
He, H., Smith, R., 1999. Stable isotope composition of water vapor in the atmospheric boundary layer above the forests of New England. J. Geophys. Res. 104, 11657–11673.
Helliker, B.R., Richter, S.L., 2008. Subtropical to boreal convergence of tree-leaf temperatures. Nature 454, 511–U6.
Herbin, H., Hurtmans, D., Turquety, S., Wespes, C., Barret, B., Hadji-Lazaro, J., Clerbaux, C., Coheur, P.-F., 2007. Global distributions of water vapour isotopologues retrieved from IMG/ADEOS data. Atmos. Chem. Phys. 7 (14), 3957–3968.
Herbstritt, B., Gralher, B., Weiler, M., 2012. Continuous in situ measurements of stable isotopes in liquid water. Water Resour. Res. 48, W03601.
Hesterburg, R., Siegenthaler, U., 1991. Production and stable isotopic composition of CO_2 in soil near Bern, Switzerland. Tellus B 43, 197–205.
Hobbie, E.A., Werner, R.A., 2004. Intramolecular, compound-specific, and bulk carbon isotope patterns in C_3 and C_4 plants: a review and synthesis. New Phytol. 161, 371–385.
Hoefs, J., 1997. Stable Isotope Geochemistry. Springer.
Hoffmann, G., Cuntz, M., Weber, C., Ciais, P., Friedlingstein, P., Heimann, M., Jouzel, J., Kaduk, J., Maier-Reimer, E., Seibt, U., Six, K., 2004. A model of the Earth's Dole effect. Glob. Biogeochem. Cycl. 18 (January (1)), GB1008.
Högberg, P., Nordgren, A., Buchmann, N., Taylor, A.F.S., Ekblad, A., Hogberg, M.N., Nyberg, G., Ottosson-Lofvenius, M., Read, D.J., 2001. Large-scale forest girdling shows that current photosynthesis drives soil respiration. Nature 411, 789–792.
Hymus, G.J., Maseyk, K., Valentini, R., Yakir, D., 2005. Large daily variation in ^{13}C-enrichment of leaf-respired CO_2 in two Quercus forest canopies. New Phytol. 167 (2), 377–384, 28.
Jassal, R., Black, T., Nesic, Z., Gaumont-Guay, D., 2012. Using automated non-steady-state chamber systems for making continuous long-term measurements of soil CO_2 efflux in forest ecosystems. Agric. Forest Meteorol. 161, 57–65.
Jung, M., Reichstein, M., Ciais, P., Seneviratne, S.I., Sheffield, J., Goulden, M.L., Bonan, G., Cescatti, A., Chen, J., de Jeu, R., Dolman, A.J., Eugster, W., Gerten, D., Gianelle, D., Gobron, N., Heinke, J., Kimball, J., Law, B.E., Montagnani, L., Mu, Q., Mueller, B., Oleson, K., Papale, D., Richardson, A.D., Roupsard, O., Running, S., Tomelleri, E., Viovy, N., Weber, U., Williams, C., Wood, E., Zaehle, S., Zhang, K., 2010. Recent decline in the global land evapotranspiration trend due to limited moisture supply. Nature 467, 951–954.
Kahmen, A., Sachse, D., Arndt, S., Tu, K., Farrington, H., Vitousek, P., Dawson, T., 2011. Cellulose $\delta^{18}O$ is an index of leaf-to-air vapor pressure difference (vpd) in tropical plants. Proc. Natl. Acad. Sci. U. S. A. 108, 1981–1986.
Kammer, A., Tuzson, B., Emmenegger, L., Knohl, A., Mohn, J., Hagedorn, F., 2011. Application of a quantum cascade laser-based spectrometer in a closed chamber system for real-time $d^{13}C$ and $d^{18}O$ measurements of soil-respired CO_2. Agr. Forest Meteorol. 151, 39–48.
Kawagucci, S., Tsunogai, U., Kudo, S., Nakagawa, F., Honda, H., Aoki, S., Nakazawa, T., Tsutsumi, M., Gamo, T., 2008. Long-term observation of mass-independent oxygen isotope anomaly in stratospheric CO(2). Atmos. Chem. Phys. 8 (20), 6189–6197.
Kayler, Z., Sulzman, E., Rugh, W., Mix, A., Bond, B., 2010. Characterizing the impact of diffusive and advective soil gas transport on the measurement and interpretation of the isotopic signal of soil respiration. Soil Biol. Biochem. 42, 435–444.
Keeling, C.D., 1958. The concentration and isotopic abundances of atmospheric carbon dioxide in rural areas. Geochim. Cosmochim. Acta 13, 322–334.
Keeling, C.D., Mook, W.G., Tans, P.P., 1979. Recent trends in the 13C–12C ratio of atmospheric carbon-dioxide. Nature 277, 121–123.
Kerstel, E., Gagliardi, G., Gianfrani, L., Meijer, H., van Trigt, R., Ramaker, R., 2002. Determination of the 2H/1H, 17O/16O and 18O/16O isotope ratios in water by means of tunable diode laser spectroscopy at 1.39 μm. Spectrochim. Acta 58, 2389–2396.

Kerstel, E., Gianfrani, L., 2008. Advances in laser-based isotope ratio measurements: selected applications. Appl. Phys. B 92, 439–449.
Kerstel, E., van Trigt, R., Dam, N., Reuss, J., Meijer, H., 1999. Simultaneous determination of the 2H/1H, 17O/16O and 18O/16O isotope abundance ratios in water by means of laser spectrometry. Anal. Chem. 71, 5297–5303.
Kljun, N., Calanca, P., Rotachhi, M.W., Schmid, H.P., 2004. A simple parameterisation for flux footprint predictions. Bound. Layer Meteorol. 112, 503–523.
Klumpp, K., Schäufele, R., Lötscher, M., Lattanzi, F.A., Feneis, W., Schnyder, H., 2005. C-isotope composition of CO_2 respired by shoots and roots: fractionation during dark respiration? Plant Cell Environ. 28, 241–250.
Kodama, N., Barnard, R.L., Salmon, Y., Weston, C., Ferrio, J.P., Holst, J., Werner, R.A., Saurer, M., Rennenberg, H., Buchmann, N., Gessler, A., 2008. Temporal dynamics of the carbon isotope composition in a *Pinus sylvestris* stand: from newly assimilated organic carbon to respired carbon dioxide. Oecologia 156, 737–750.
Lai, C.T., Schauer, A.J., Owensby, C., Ham, J.M., Ehleringer, J.R., 2003. Isotopic air sampling in a tallgrass prairie to partition net ecosystem CO2 exchange. J. Geophys. Res.-Atmos. 108 (D18), http://dx.doi.org/10.1029/2002JD003369, Art. No. 4566.
Lai, C., Ehleringer, J., Bond, B.U.K., 2006. Contributions of evaporation, isotopic non-steady state transpiration and atmospheric mixing on the delta O-18 of water vapour in Pacific Northwest coniferous forests. Plant Cell Environ. 29, 77–94.
Lee, X., 2003. Fetch and footprint of turbulent fluxes over vegetative stands with elevated sources. Bound. Layer Meteorol. 107 (3), 561–579.
Lee, X., Griffis, T., Baker, J., Billmark, K., Kim, K., Welp, L., 2009. Canopy-scale kinetic fractionation of atmospheric carbon dioxide and water vapor isotopes. Glob. Biogeochem. Cycl. 23, GB1002.
Lee, X., Huang, J., Patton, E., 2012. A large-eddy simulation study of water vapour and carbon dioxide isotopes in the atmospheric boundary layer. Bound. Layer Meteorol. 145, 229–248.
Lee, X., Sargent, S., Smith, R., Tanner, B., 2005. In-situ measurement of the water vapor $^{18}O/^{16}O$ isotope ratio for atmospheric and ecological applications. J. Atmos. Ocean. Technol. 22, 555–565.
Lee, X., Smith, R., Williams, J., 2006. Water vapour 18O/16O isotope ratio in surface air in New England, USA. Tellus B 58, 293–304.
Lee, X.H., Kim, K., Smith, R., 2007. Temporal variations of the $^{18}O/^{16}O$ signal of the whole-canopy transpiration in a temperate forest. Glob. Biogeochem. Cycl. 21 (3), GB3013, http://dx.doi.org/10.1029/2006GB002871.
Leen, J., Berman, E., Liebson, L., Gupta, M., 2012. Spectral comtaminant identifier for off-axis integrated cavity output spectroscopy measurements of liquid water isotopes. Rev. Sci. Instrum. 83, 044305.
Lin, G.H., Ehleringer, J.R., 1997. Carbon isotopic fractionation does not occur during dark respiration in C_3 and C_4. Plant Physiol. 114 (1), 391–394.
Livingston, G., Hutchinson, G., 1995. Enclosure based measurements of trace gas exchange: applications and sources of error. In: Biogenic Trace Gases: Measuring Emissions from Soil and Water. Blackwell Science, Malden, pp. 14–51.
Maseyk, K., Wingate, L., Seibt, U., Ghashghaie, J., Bathellier, C., Almeida, P., de Vale, R.L., Pereira, J.S., Yakir, D., Mencuccini, M., 2009. Biotic and abiotic factors affecting the delta C-13 of soil respired CO_2 in a Mediterranean oak woodland. Isot. Environ. Health Stud. 45, 343–359.
Massman, W., Ibrom, A., 2008. Attenuation of concentration fluctuations of water vapor and other trace gases in turbulent flow. Atmos. Chem. Phys. 8, 6245–6259.
McAlexander, I., Rau, G., Liem, J., Owano, T., Fellers, R., Baer, D., Gupta, M., 2011. Deployment of a carbon isotope ratiometer for the monitoring of CO_2 sequestration leakage. Anal. Chem. 83, 6223–6229.
McDowell, N.G., Bowling, D.R., Bond, B.J., et al., 2004. Response of the carbon isotopic content of ecosystem, leaf, and soil respiration to meteorological and physiological driving factors in a Pinus ponderosa ecosystem. Global Biogeochem. Cy. 18, GB1013, http://dx.doi.org/10.1029/2003GB002049.
McKinney, C., McCrea, J., Epstein, S., Allen, H., 1950. Improvements in mass spectrometers for the measurement of small differences in isotope abundance ratios. Rev. Sci. Instrum. 21, 724–730.
Midwood, A., Millard, P., 2011. Challenges in measuring the $\delta^{13}C$ of the soil surface CO_2 efflux. Rapid Commun. Mass Spectrom. 25, 232–242.
Miller, J.B., Tans, P.P., White, J.W.C., Conway, T.J., Vaughn, B.W., 2003. The atmospheric signal of terrestrial carbon isotopic discrimination and its implication for partitioning carbon fluxes. Tellus B 55, 197–206.
Mohn, J., Zeeman, M., Werner, R., Eugster, W., Emmenegger, L., 2008. Continuous field measurement of $\delta^{13}C$–CO_2 and trace gases by FTIR spectroscopy. Isot. Environ. Health Stud. 44, 241–251.
Morgenstern, K., Black, T.A., Humphreys, E.R., Griffis, T.J., Drewitt, G.B., Cai, T.B., Nesic, Z., Spittlehouse, D.L., Livingstone, N.J., 2004. Sensitivity and uncertainty of the carbon balance of a Pacific Northwest Douglas-fir forest during an El N ino La N ina cycle. Agric. Forest Meteorol. 123 (3–4), 201–219, 57.
Mortazavi, B., Chanton, J.P., 2002. Carbon isotopic discrimination and control of nighttime canopy $\delta^{18}O$–CO_2 in a pine forest in the southeastern United States. Glob. Biogeochem. Cycl. 16, http://dx.doi.org/10.1029/2000GB001390.
Murphey, B., Nier, A., 1941. Variations in the relative abundance of the carbon isotopes. Phys. Rev. 59, 771–772.
Nier, A., Gulbransen, E., 1939. Variations in the relative abundance of the carbon isotopes. J. Am. Chem. Soc. 61, 697–698.
Nier, A.O., 1947. A mass spectrometer for isotope and gas analysis. Rev. Sci. Instrum. 19 (6), 398–411.
Ogée, J., Barbour, M.M., Wingate, L., Bert, D., Bosc, A., Stievenard, M., Lambrot, C., Pierre, M., Bariac, T., Loustau, D., Dewar, R.C., 2009. A single-substrate model to interpret intra-annual stable isotope signals in tree-ring cellulose. Plant Cell Environ. 32 (August (8)), 1071–1090.
Ogée, J., Brunet, Y., Loustau, D., Berbigier, P., Delzon, S., 2003. MuSICA, a CO_2, water and energy multilayer, multileaf pine forest model: evaluation from hourly to yearly time scales and sensitivity analysis. Glob. Change Biol. 9 (5), 697–717.
Ogée, J., Cuntz, M., Peylin, P., Bariac, T., 2007. Non-steady-state, non-uniform transpiration rate and leaf anatomy effects on the progressive stable isotope enrichment of leaf water along monocot leaves. Plant Cell Environ. 30 (April (4)), 367–387.
Ogée, J., Peylin, P., Cuntz, M., Bariac, T., Brunet, Y., Berbigier, P., Richard, P., Ciais, P., 2004. Partitioning net ecosystem carbon exchange into net assimilation and respiration with canopy-scale isotopic measurements: an error propagation analysis with $^{13}CO_2$ and $CO^{18}O$ data. Glob. Biogeochem. Cycl. 18 (2), 16–34.
Pataki, D.E., Ehleringer, J.R., Flanagan, L.B., Yakir, D., Bowling, D.R., Still, C.J., Buchmann, N., Kaplan, J.O., Berry, J.A., 2003. The application and interpretation of Keeling plots in terrestrial carbon cycle research. Glob. Biogeochem. Cycles 17 (1), Art. No. 1022.
Plain, C., Gerant, D., Maillard, P., Dannoura, M., Dong, Y., Zeller, B., Priault, P., Parent, F., Epron, D., 2009. Tracing of recently assimilated carbon in respiration at high temporal resolution in the field with a tuneable diode laser absorption spectrometer after in situ 13CO2 pulse labelling of 20-year-old beech trees. Tree Physiol. 29, 1433–1445.
Ponton, S., Flanagan, L.B., Alstad, K.P., Johnson, B.G., Morgenstern, K., Kljun, N., Black, T.A., Barr, A.G., 2006. Comparison of ecosystem water-use efficiency among Douglas-fir forest, aspen forest and grassland using eddy covariance and carbon isotope techniques. Glob. Change Biol. 12, 294–310.
Powers, H.H., Hunt, J.E., Hanson, D.T., McDowell, N.G., 2010. A dynamic soil chamber system coupled with a tunable diode laser for online measurements of delta C-13, delta O-18, and efflux rate of soil-respired CO_2. Rapid Commun. Mass Spectrom. 24, 243–253.
Rambo, J., Lai, C.-T., Farlin, J., Schroeder, M., Bible, K., 2012. On-site calibration for high precision measurements of water vapor isotope ratios using off-axis cavity-enhanced absorption spectroscopy. J. Atmos. Ocean. Technol. 28, 1448–1457.
Randerson, J.T., Collatz, G.J., Fessenden, J.E., Munoz, A.D., Still, C.J., Berry, J.A., Fung, I.Y., Suits, N., Denning, A.S., 2002. A possible global covariance between terrestrial gross primary production and C-13 discrimination: consequences for the atmospheric C-13 budget and its response to enso 6. Glob. Biogeochem. Cycl. 16 (4), 1136, http://dx.doi.org/10.1029/2001GB001845.
Riley, W.J., Still, C.J., Helliker, B.R., Ribas-Carbo, M., Berry, J.A., 2003. O-18 composition of CO_2 and H_2O ecosystem pools and fluxes in a tallgrass prairie: simulations and comparisons to measurements. Glob. Change Biol. 9, 1567–1581.
Riley, W.J., Still, C.J., Torn, M.S., Berry, J.A., 2002. A mechanistic model of (H_2O)-O-18 and (COO)-O-18 fluxes between ecosystems and the atmosphere: model description and sensitivity analyses. Glob. Biogeochem. Cycl. 16, 1095.
Risk, D., Kellman, L., 2008. Isotopic fractionation in non-equilibrium diffusive environments. Geophys. Res. Lett., 35.
Risk, D., Nickerson, N., Phillips, C.L., Kellman, L., Moroni, M., 2012. Drought alters respired delta(CO_2)-C-13 from autotrophic, but not heterotrophic soil respiration. Soil Biol. Biochem. 50, 26–32.
Rochette, P., Flanagan, L.B., 1999. Quantifying rhizosphere respiration in a corn crop under field conditions. Soil Sci. Soc. Am. 61, 466–474.
Saleska, S.R., Shorter, J.H., Herndon, S., Jimenez, R., McManus, B., Munger, J.W., Nelson, D.D., Zahniser, M.S., 2006. What are the instrumentation requirements for measuring the isotopic composition of net ecosystem exchange of CO_2 using eddy covariance methods? Isot. Environ. Health Stud. 42 (2), 115–133, 46.
Santoni, G.W., Lee, B.H., Goodrich, J.P., Varner, R.K., Crill, P.M., McManus, J.B., Nelson, D.D., Zahniser, M.S., Wofsy, S.C., 2012. Mass fluxes and isofluxes of methane (CH_4) at a New Hampshire fen measured by a continuous wave quantum cascade laser spectrometer. J. Geophys. Res. Atmos. 117, http://dx.doi.org/10.1029/2011JD016960.
Santos, E., Wagner-Riddle, C., Lee, X., Warland, J., Brown, S., Staebler, R., Bartlet, P., Kim, K., 2012. Use of the isotope flux ratio approach to investigate the C18O16O and $13CO_2$ exchange near the floor of a temperate deciduous forest. Biogeosciences 9, 2385–2399.
Schaeffer, S.M., Miller, J.B., Vaughn, B.H., White, J.W.C., Bowling, D.R., 2008. Long-term field performance of a tunable diode laser absorption spectrometer for analysis of carbon isotopes of CO_2 in forest air. Atmos. Chem. Phys. Discuss. 8 (3), 9531–9568.
Schiff, H., 1992. Ground based measurements of atmospheric gases by spectroscopic methods. Berichte der Bunsengesellschaft für physikalische Chemie 96, 296–306.
Schiff, H., 1994. The measurement of trace gases using ground-based instrumentation. In: Chemistry of the Atmosphere. CRC Press.
Schultz, N., Griffis, T., Lee, X., Baker, J., 2011. Identification and correction of spectral contamination in 2H/1H and 18O/16O measured in leaf, stem, and soil water. Rapid Commun. Mass Spectrom. 25, 3360–3368.
Seibt, U., Wingate, L., Lloyd, J., Berry, J.A., 2006. Diurnally variable $\delta^{18}O$ signatures of soil CO_2 fluxes indicate carbonic anhydrase activity in a forest soil. J. Geophys. Res. Biogeosci. 111 (November (G4)), G04005, http://dx.doi.org/10.1029/2006JG000177.
Simpson, T.J., 1998. Application of isotopic methods to secondary metabolic pathways. Biosynthesis 195, 1–48.
Soddy, F., 1913. The radioelements and the periodic law. Chem. News 107, 97.
Sternberg, L., Moreira, M., Martinelli, L., Victoria, R., Barbosa, E., Bonates, L., Nepstad, D., 1998. The relationship between O-18/O-16 and C-13/C-12 ratios of ambient CO_2 in two Amazonian tropical forests. Tellus B 50 (September (4)), 366–376.

Sturm, P., Eugster, W., Knohl, A., 2012. Eddy covariance measurements of CO_2 isotopologues with a quantum cascade laser absportion spectrometer. Agric. Forest Meteorol. 152, 73–82.
Sturm, P., Knohl, A., 2009. Water vapor δ^2H and $\delta^{18}O$ measurements using off-axis integrated cavity output spectroscopy. Atmos. Measur. Tech. Discuss. 2, 2055–2085.
Tans, P.P., Fung, I.Y., Takahashi, T., 1990. Observation constraints on the global atmospheric CO_2 budget. Science 247, 1431–1438.
Tazoe, Y., Von Caemmerer, S., Estavillo, G.M., Evans, J.R., 2011. Using tunable diode laser spectroscopy to measure carbon isotope discrimination and mesophyll conductance to CO_2 diffusion dynamically at different CO_2 concentrations. Plant Cell Environ. 34 (April (4)), 580–591.
Tcherkez, G., Farquhar, G.D., Badeck, F., Ghashghaie, J., 2004. Theoretical considerations about carbon isotope distribution in glucose of C_3 plants. Funct. Plant Biol. 31 (9), 857–877.
Tcherkez, G., Nogués, S., Bleton, J., Cornic, G., Badeck, F.W., Ghashghaie, J., 2003. Metabolic origin of carbon isotope composition of leaf dark-respired CO_2 in French bean. Plant Physiol. 131, 237–244.
Thiemens, M., 1999. Mass-independent isotope effects in planetary atmospheres and the early solar system. Science 283, 341–345.
Thomson, J., 1913. the appearance of helium and neon in vacuum tubes. Nature 90, 645.
Trolier, M., White, J.W.C., Tans, P.P., Masarie, K.A., Gemery, P.A., 1996. Monitoring the isotopic composition of atmospheric CO_2: measurements from the noaa global air sampling network. J. Geophys. Res. Atmos. 101 (D20), 25897–25916.
Trumbore, S., 2006. Carbon respired by terrestrial ecosystems – recent progress and challenges. Glob. Change Biol. 12, 141–153.
Tuzson, B., Mohn, J., Zeeman, M., Werner, R., Eugster, W., Zahniser, M., Nelson, D., McManus, J., Emmenegger, L., 2008. High precision and continuous field measurements of $\delta^{13}C$ and $\delta^{18}O$ in carbon dioxide with a cryogen-free QCLAS. Appl. Phys. B 92, 451–458.
Urey, H., 1948. Oxygen isotopes in nature and in the laboratory. Science 108, 489–496.
Urey, H., Brickwedde, Murphy, 1932. A hydrogen isotope of mass 2 and its concentration. Phys. Rev. 40, 1–15.
Vogel, F., Huang, L., Ernst, D., Giroux, L., Racki, S., Worthy, D., 2012. Evaluation of a cavity ring-down spectrometer for in-situ observations of 13CO. Atmos. Measur. Tech. Discuss. 5, 6037–6058.
Wagner-Riddle, C., Thurtell, G.W., Edwards, G.C., 2005. Trace gas concentration measurements for micrometeorological flux quantification. In: Micrometeorology in Agricultural Systems. Agronomy Monography No. 47, American Society of Agronomy, Madison, WI, USA, pp. 321–344.
Wahl, E.H., Fidric, B., Rella, C.W., Koulikov, S., Kharlamov, B., Tan, S., Kachanov, A.A., Richman, B.A., Crosson, E.R., Paldus, B.A., Kalaskar, S., Bowling, D.R., 2006. Applications of cavity ring-down spectroscopy to high precision isotope ratio measurement of C-13/C-12 in carbon dioxide. Isot. Environ. Health Stud. 42 (March (1)), 21–35.
Wang, L., Caylor, K., Villegas, J., Barron-Gafford, G., Breshears, D., Huxman, T., 2010. Partitioning evapotranspiration across gradients of woody plant cover: assessment of a stable isotope technique. Geophys. Res. Lett. 37, L09401.
Wang, L., Good, S., Caylor, K., Cernusak, L., 2012. Direct quantification of leaf transpiration isotopic composition. Agric. Forest Meteorol. 154–155, 127–135.
Wang, L.X., Caylor, K.K., Dragoni, D., 2009. On the calibration of continuous, high-precision delta(18)O and delta(2)H measurements using an off-axis integrated cavity output spectrometer. Rapid Commun. Mass Spectrom. 23, 530–536.
Welp, L., Keeling, R., Meijer, H., Bollenbacher, A., Piper, S., Yoshimura, K., Francey, R., Allison, C., Wahlen, M., 2011. Interannual variability in the oxygen isotopes of atmospheric CO_2 driven by el nino. Nature 477, 579–582.
Welp, L., Lee, X., Griffis, T., Wen, X., Xiao, W., Li, S., Sun, X., Hu, Z., Martin, M.V., Huang, J., 2012. A meta-analysis of water vapor deuterium-excess in the midlatitude atmospheric surface layer. Glob. Biogeochem. Cycl. GB3021, 1–12.
Welp, L.R., Lee, X., Kim, K., Griffis, T.J., Billmark, K.A., Baker, J.M., 2008. $\delta^{18}O$ of water vapour, evapotranspiration and the sites of leaf water evaporation in a soybean canopy. Plant Cell Environ. 31 (September (9)), 1214–1228.
Wen, X., Lee, X., Sun, X., Wang, J., Li, S., Yu, G., 2012. Inter-comparison of four commercial analyzers for water vapor isotope measurement. J. Atmos. Ocean. Technol. 29, 235–247.
Wen, X.-F., Meng, Y., Zhang, X.-Y., Sun, X.-M., Lee, X., 2013. Evaluating calibration strategies for isotope ratio infrared spectroscopy for atmospheric $^{13}CO_2/^{12}CO_2$ measurement. Atmos. Meas. Tech. Discuss. 6, 795–823.
Wen, X.-F., Sun, X.-M., Zhang, S.-C., Yu, G.-R., Sargent, S.D., Lee, X., 2008. Continuous measurement of water vapor D/H and O-18/O-16 isotope ratios in the atmosphere. J. Hydrol. 349 (February (3–4)), 489–500.
Werle, P., 2004. Diode-laser sensors for in-situ gas analysis. In: Lasers in Environmental and Life Sciences – Modern Analytical Methods. Springer-Verlag, pp. 223–243.
Werle, P., 2011. Accuracy and precision of laser spectrometers for trace gas sensing in the presence of optical fringes and atmospheric turbulence. Appl. Phys. B: Lasers Opt. 102, 313–329.
Werle, P., Mucke, R., Slemr, F., 1993. The limits of signal averaging in atmospheric trace-gas monitoring by tunable diode-laser absorption-spectroscopy (tdlas). Appl. Phys. B: Photophys. Laser Chem. 57, 131–139.
Werner, C., Gessler, A., 2011. Diel variations in the carbon isotope composition of respired CO_2 and associated carbon sources: a review of dynamics and mechanisms. Biogeosciences 8, 2437–2459.
Werner, C., Schnyder, H., Cuntz, M., Keitel, C., Zeeman, M., Dawson, T., Badeck, W., Brugnoli, E., Ghashghaie, J., Grams, T., Kayler, Z., Lakatos, M., Lee, X., Máguas, C., Ogée, J., Rascher, K., Siegwolf, R., Unger, S., Welker, J., Wingate, L., Gessler, A., 2012. Progress and challenges using stable isotopes to trace plant carbon and water relations across scales. Biogeosciences 9, 3083–3111.
West, A.G., Goldsmith, G., Brooks, P., Dawson, T., 2010. Discrepancies between isotope ratio infrared spectroscopy and isotope ratio mass spectrometry for the stable isotope analysis of plant and soil waters. Rapid Commun. Mass Spectrom. 24, 1948–1954.
Williams, D., Cable, W., Hultine, K., Hoedjes, J., Yepez, E., Simonneaux, V., Er-Raki, S., Boulet, G., de Bruin, H., Chehbouni, A., Hartogensis, O., Timouk, F., 2004. Evapotranspiration components determined by stable isotope, sap flow and eddy covariance techniques. Agric. Forest Meteorol. 125, 241–258.
Wingate, L., Ogée, J., Burlett, R., Bosc, A., 2010a. Strong seasonal disequilibrium measured between the oxygen isotope signals of leaf and soil CO_2 exchange. Glob. Change Biol. 16, 3048–3064.
Wingate, L., Ogee, J., Burlett, R., Bosc, A., Devaux, M., Grace, J., Loustau, D., Gessler, A., 2010b. Photosynthetic carbon isotope discrimination and its relationship to the carbon isotope signals of stem, soil and ecosystem respiration. New Phytol. 188 (2), 576–589.
Wingate, L., Ogee, J., Cuntz, M., Genty, B., Reiter, I., Seibt, U., Yakir, D., Maseyk, K., Pendall, E.G., Barbour, M.M., Mortazavi, B., Burlett, R., Peylin, P., Miller, J., Mencuccini, M., Shim, J.H., Hunt, J., Grace, J., 2009. The impact of soil microorganisms on the global budget of delta O-18 in atmospheric CO_2. Proc. Natl. Acad. Sci. U. S. A. 106, 22411–22415.
Worden, J., Bowman, K., Noone, D., Beer, R., Clough, S., Eldering, A., Fisher, B., Goldman, A., Gunson, M., Herman, R., Kulawik, S.S., Lampel, M., Luo, M., Osterman, G., Rinsland, C., Rodgers, C., Sander, S., Shephard, M., Worden, H., 2006. Tropospheric emission spectrometer observations of the tropospheric HDO/H_2O ratio: estimation approach and characterization. J. Geophys. Res. Atmos. 111, http://dx.doi.org/10.1029/2005JD006606.
Worden, J., Noone, D., Bowman, K., 2007. Importance of rain evaporation and continental convection in the tropical water cycle. Nature 445, 528–532.
Xiao, W., Lee, X., Griffis, T., Kim, K., Welp, L., Yu, Q., 2010. A modeling investigation of canopy-air oxygen isotopic exchange of water vapor and carbon dioxide in a soybean field. J. Geophys. Res. Biogeosci. 115, G01004, http://dx.doi.org/10.1029/2009JG001163.
Xiao, W., Lee, X., Wen, X., Sun, X., Zhang, S., 2012. Modeling biophysical controls on canopy foliage water 18O enrichment in wheat and corn. Glob. Change Biol. 18, 1769–1780.
Xu, L.K., Baldocchi, D.D., 2004. Seasonal variation in carbon dioxide exchange over a mediterranean annual grassland in California. Agric. Forest Meteorol. 123 (1–2), 79–96.
Yakir, D., 2003. The stable isotopic composition of atmospheric CO_2. In: Holland, H.D., Turekian, K.K. (Eds.), In: The Atmosphere, Treatise on Geochemistry, vol. 4. Elsevier-Pergamon, Oxford, pp. 175–212 (Chapter 4.07).
Yakir, D., Sternberg, L.D.L., 2000. The use of stable isotopes to study ecosystem gas exchange. Oecologia 123, 297–311.
Yakir, D., Wang, X.F., 1996. Fluxes of CO_2 and water between terrestrial vegetation and the atmosphere estimated from isotope measurements. Nature 380, 515–517.
Yepez, E., Williams, D., Scott, R., Lin, G., 2003. Partitioning overstory and understory evapotranspiration in a semiarid savanna woodland from the isotopic composition of water vapor. Agric. Forest Meteorol. 119, 53–68.
Yilmaz Jr., M., Jackson, E.H.T., 2008. Remote sensing of vegetation water content from equivalent water thickness using satellite imagery. Remote Sens. Environ. 112, 2514–2522.
Zhang, J., Griffis, T.J., Baker, J.M., 2006. Using continuous stable isotope measurements to partition net ecosystem CO_2 exchange. Plant Cell Environ. 29 (4), 483–496.
Zhao, L.J., Xiao, H.L., Zhou, J., Wang, L.X., Cheng, G.D., Zhou, M.X., Yin, L., McCabe, M.F., 2011. Detailed assessment of isotope ratio infrared spectroscopy and isotope ratio mass spectrometry for the stable isotope analysis of plant and soil waters rid a-2572-2008 rid g-5194-2011. Rapid Commun. Mass Spectrom. 25, 3071–3082.
Zobitz, J.M., Burns, S.P., Ogée, J., Reichstein, M., Bowling, R., 2007. Partitioning net ecosystem exchange of CO_2: a comparison of a Bayesian/isotope approach to environmental regression methods. J. Geophys. Res. Biogeosci. 112 (G3).
Zobitz, J.M., Keener, J.P., Schnyder, H., Bowling, D.R., 2006. Sensitivity analysis and quantification of uncertainty for isotopic mixing relationships in carbon cycle research. Agric. Forest Meteorol. 136 (1–2), 56–75, 43.